8-2008

Dispersion of narrow diameter carbon nanotubes for optical characterization.

Hemant M. Shah 1981-
University of Louisville

DISPERSION OF NARROW DIAMETER CARBON NANOTUBES FOR OPTICAL CHARACTERIZATION

By

Hemant M. Shah
B.S.,Maharaja Sayajirao University, Baroda, Gujarat, India

A Thesis
Submitted to the Faculty of the
Graduate School of the University of Louisville
In Partial fulfillment of the requirements
For the degree of

Master of Science

Department of Electrical and Computer Engineering
University of Louisville
Louisville, Kentucky

August, 2008

DISPERSION OF NARROW DIAMETER CARBON NANOTUBES FOR OPTICAL CHARACTERIZATION

By

Hemant M. Shah

B.S., Maharaja Sayajirao University, Baroda, Gujarat, India

A Thesis Approved on

August 7th, 2007

By the following Thesis Committee

_____

Dr. Bruce W. Alphenaar (Thesis Director)

_____

Dr. Robert W. Cohn

_____

Dr. Gamini Sumanasekara

DEDICATION

This thesis is dedicated to my parents

Mr. Mahesh K. Shah

&

Mrs. Gopi M. Shah

who have always guided me and shown me the right path, encouraged me during my tough times to accomplish my dreams. They have been my biggest inspiration and supported me in every path of my life.

I would also like to dedicate this thesis to my sister who is an integral part of my life.

ACKNOWLEDGEMENTS

ABSTRACT

DISPERSION OF NARROW DIAMETER CARBON NANOTUBES

FOR OPTICAL CHARACTERIZATION

Hemant M. Shah

August 7th, 2007

Optical properties of carbon nanotubes have recently attracted considerable amount of attention. Due to there direct band gap material characteristic these and dimension of the order of nano meters they find potential applications in the field of nano photonics. Thus the optical study of carbon nanotubes is important for both fundamental research and for the next generation technical applications.

In this thesis single walled carbon nanotubes were dispersed in various encapsulates such as surfactants, polymers, proteins etc to separate them individually and study there optical properties. The individually dispersed single walled carbon nanotubes displayed unique absorbance spectra. The optical absorption spectrum of a particular tube is expected to be dominated by a series of relatively sharp inter-band transitions, at energies associated with the van Hove singularities, the absorbance spectrum obtained on our samples were consistent with this expectation. Our samples also showed sharp photoluminescence peaks mostly from the semiconducting single walled carbon nanotubes. The detailed

overlap of the absorbance spectra and photoluminescence spectra lead us to believe that our samples contain mainly individual tubes encapsulated in one of the surfactants or polymers. Thin film transistors (TFT) were made with a mesh of single walled carbon nanotubes as the active channel on top of a silicon/silicon oxide substrate, with silicon acting as a back gate and titanium/gold electrodes were evaporated on top of the nanotube film. Photocurrent properties of these thin films were investigated and they showed a huge change in the photocurrent in the presence and absence of the laser light. Thin films of carbon nanotubes were also deposited on rectangular silicon substrates and the influence of applied strain in the presence of laser light was investigated. These films showed a huge change in resistance on application of mechanical strain. Raman measurements were also performed on these thin films and the obtained radial breathing mode (RBM) data helped resolve the diameter of many single walled carbon nanotubes.

TABLE OF CONTENTS

PAGE

LIST OF TABLES

TABLE   **PAGE**

LIST OF FIGURES

x

CHAPTER I

INTRODUCTION

1.1 Nanotechnology

Nanotechnology is the study and control of matter on a small scale (less than 1 micrometer). It is a multidisciplinary field where varying disciplines from fundamental science to pure engineering work together. Special analytical tools such as the AFM (atomic force microscope), SEM (scanning electron microscope), and TEM (tunneling electron microscope) are used to study the properties of the different nanoscale materials. Efforts are also underway to explore the potential applications of different materials at the nano scale.

1.1 An Outline of this Thesis

Optical properties of single walled carbon nanotubes such as absorption and photoluminescence can be observed if they are grown directly across micro pillars or suspended in liquid encapsulants. In this thesis as-purchased carbon nanotubes were suspended in a liquid solution and their optical properties were measured. Optically active thin films of carbon nanotube were made from these solutions and photocurrent was measured on them. These films also showed significant gate dependence in a thin film transistor (TFT) device configuration. The thesis is arranged as follows: chapter two describes optical and electrical

1

properties of carbon nanotubes; chapter three explains the recipe used for suspending nanotubes in liquid solutions using different encapsulants and optical spectroscopy measurements (Raman measurements, absorbance and photoluminescence); chapter four describes the photocurrent and gate dependence measurements on single wall carbon nanotube thin film devices; chapter five concludes the thesis.

CHAPTER II

CARBON NANOTUBES

2.1 Introduction

A carbon nanotube is a one-atom thick sheet of graphene rolled up as a seamless cylinder with a diameter on the order of a nanometer. Carbon nanotubes have some of the original properties inherited from the parent in-plane graphite and a set of additional properties due to their small dimensions. Carbon nanotubes have unique optical, electronic, thermal and structural properties that change depending on the type of nanotube (defined by the chirality, diameter and length). They are claimed to have a Young's modulus higher than that of steel [1]. Their unique electronic properties have made them a very important part of the next generation of electronic devices. Carbon nanotubes for the first time represent a carbon fiber, the structure of which is entirely known, down to the atomic level [2].

There are two types of nanotubes: multi-walled carbon nanotubes (MWNTs) (discovered in 1991) and single walled carbon nanotubes (SWNTs) (discovered in 1993). MWNTs are multiple sheets of graphene rolled together to form a tube structure. They can be classified in two categories: Russian doll and parachute. The Russian doll model has a single walled nanotube within a larger

diameter tube. The parachute model has a single walled nanotube rolled around itself with several turns, similar to a parachute or a rolled paper. The diameter of MWNTs is anywhere between 20 nm to a couple of hundred nanometers. Their lengths could be a couple of hundreds of microns. As the name suggests, a single walled carbon nanotube is just one layer of graphene rolled to form a seamless cylinder. The diameter of SWNTs is about 1nm. The length of nanotubes could also be a couple of hundreds of microns. SWNTs as long as 4cm have also been reported [3].

2.2 History of Carbon Nanotubes

Carbon nanotubes were discovered by Sumio Iijima in 1991 using a high resolution transmission electron microscope [4]. These structures were given the name "carbon nanotubes" due to the fact that their diameters were of the order of few nanometers and they are rolled like a cylinder. However, carbon nanotubes had been discovered 30 years earlier by Roger Bacon [5] at Union Carbide. Carbon nanotubes did not gain attention at that time because they were supposed to be structurally imperfect.

Bacon used an arc-discharge setup under high pressure of an inert gas, where as Iijima used the same arc-discharge setup but with a low pressure. Nanotubes attracted attention after Iijima's discovery and it was realized that these tubes could be grown using different metal catalysts. The tubes identified by Iijima were actually multi-wall nanotubes, which are carbon nanotubes layered on top of other nanotubes or rolled upon a single walled nanotube, similar to a parachute.

4

It was in 1993 when Iijima along with Toshinari Ichihashi [6] also of NEC and Donald Bethune [7] at IBM working independently discovered Single-wall nanotubes using arc-discharge method in the presence of a metal catalyst. This discovery shifted the focus from multi-wall to single-wall nanotubes. However the arc-discharge method resulted in more sooth than the nanotubes thus affecting the purity of the nanotubes. It was not until Smalley and his co-workers in late 1995 discovered a more efficient synthesis process involving laser ablation method [8]. Over time, many different methods have been developed and other methods of growth are still under investigation to get the desired type or family of tubes, having unique qualities.
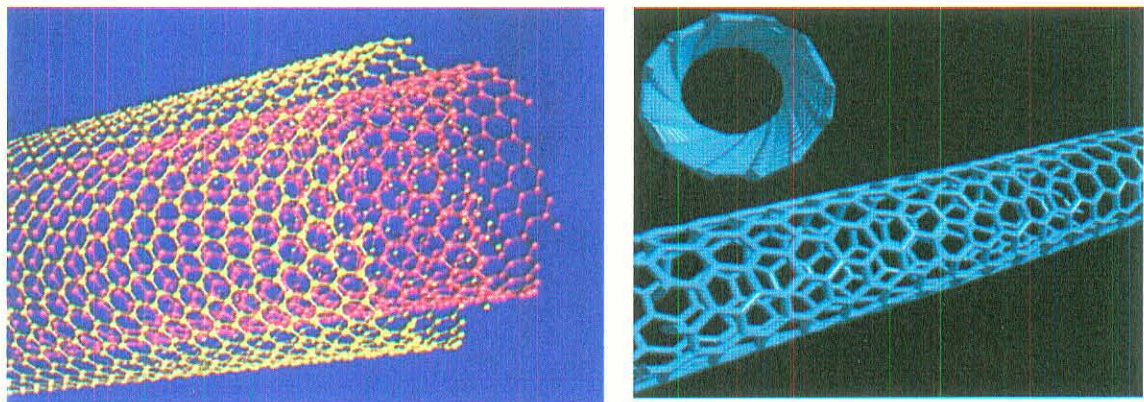
(a)   (b)

Fig 2.1 (a) Multiwalled Carbon Nanotube (b) Single Walled Carbon Nanotube.

2.3 Carbon Nanotube Growth

There are various methods by which Carbon Nanotubes can be grown. The main methods are **(a) Arc Discharge, (b) Laser Ablation and (c) Chemical Vapor Deposition.** Nanotubes grown by the chemical vapor deposition (CVD) process are considered to have better advantages compared to the other two methods. The factors that are to be considered in the growth process are the simplicity of growth, cost of the process, yield and the efficiency. The detailed mechanism responsible for the growth of these nanotubes is not yet well understood, and is the subject of intense study. Multi-walled nanotubes require no catalysts for their growth whereas single-walled nanotubes require catalytic species. The nanotubes used in this thesis were purchased from Carbon Nanotechnologies Inc and Southwest Nanotechnologies Inc. They were CVD (chemical vapor deposition) grown and 95 % pure.

2.4 Structure of Nanotubes

Depending on the way these nanotubes are rolled they can form different types; armchair, zigzag, chiral. These tubes are defined by the chiral vector (n, m), where n and m are integer values of the equation $R = na_1 + ma_2$.

Armchair: n = m

Zigzag : (n, 0)

Chiral: (n, m) m≠0
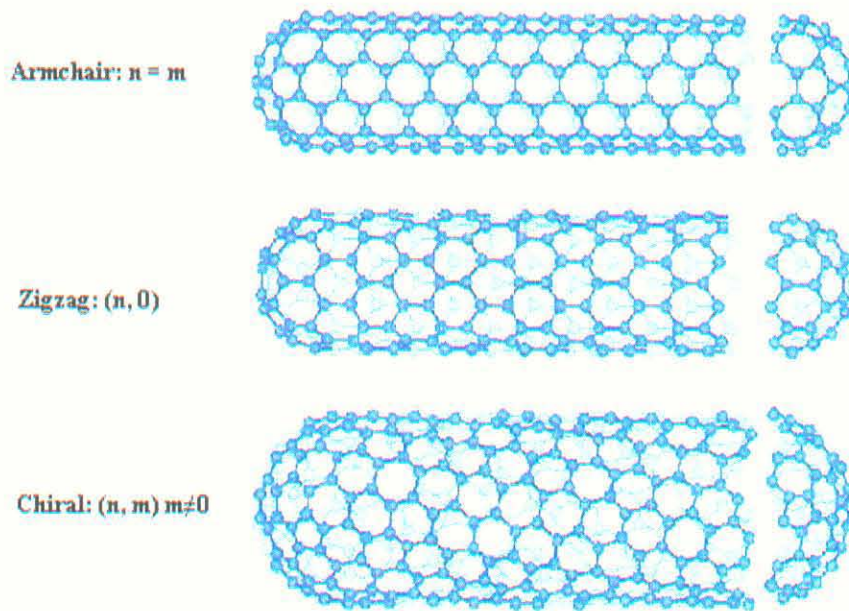
Fig 2.2 armchair, zigzag and chiral nanotube

When a graphene sheet is rolled to form the cylindrical part of the nanotube, the ends of the chiral vector meet.

2.4.1 Chiral Vector

Chirality of carbon nanotubes is defined by the chiral vector. The chiral vector thus forms the circumference of the nanotubes circular cross-section, and different values of n and m lead to armchair, zigzag or chiral nanotube. Depending on the values of n and m, these nanotubes could be either metallic or semiconducting.

(a)   (b)
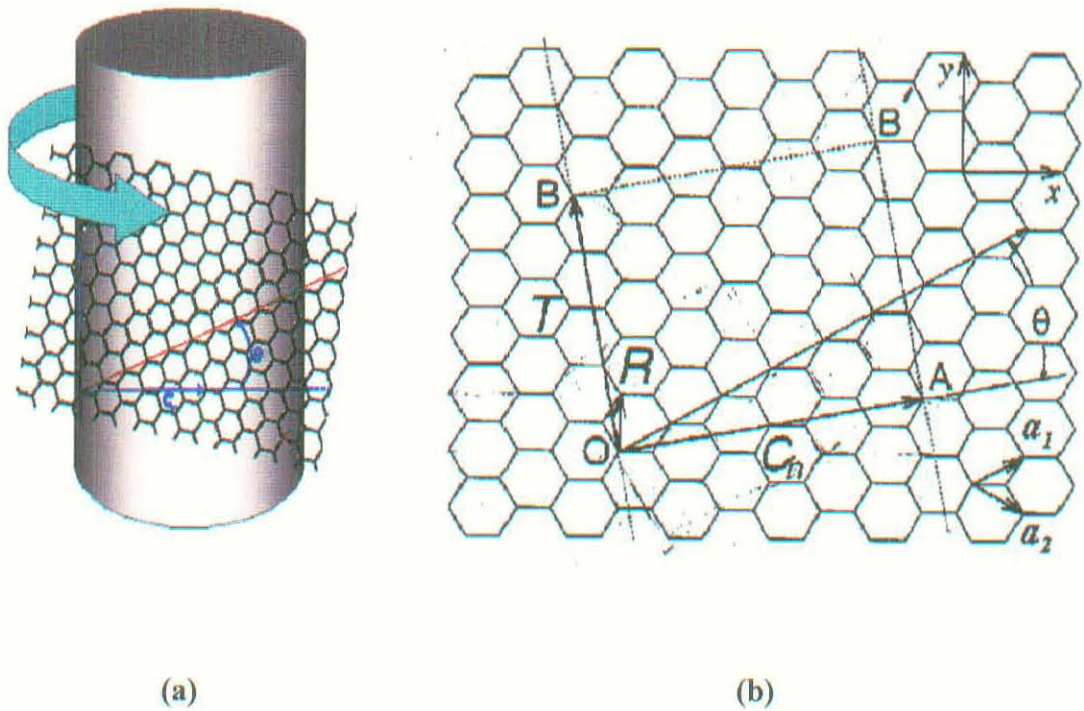
Fig 2.3: (a) carbon nanotube (b) 2d projection

As shown in Fig 2.3 (b), the vector OA is perpendicular to the nanotube axis and vector OB is along the nanotube axis. In 2D projection, when points O and B coincide and when points A and B coincide, the result is carbon nanotube structure. Depending on the value of the chiral vector these tubes are classified as armchair, zigzag or chiral.
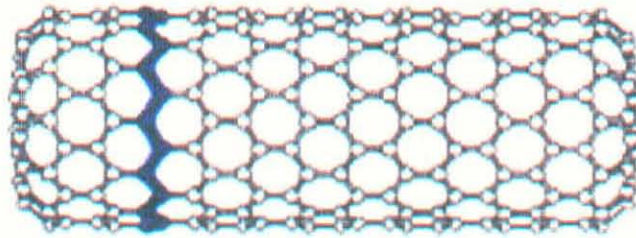
Fig 2.3.1 (n, 0) or (m, 0) Zigzag Tube
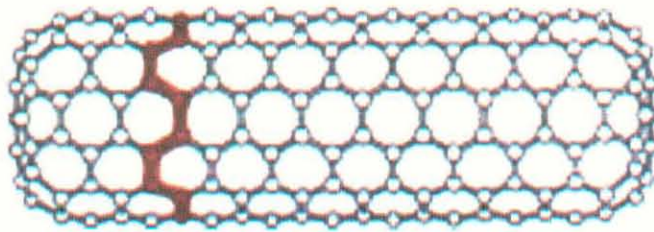
Fig 2.3.2 (n,n) Armchair Tube
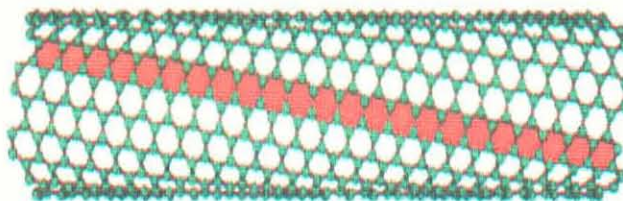
Fig 2.3.3 (n,m) Chiral Tube

The figures above show 3 different structures of carbon nanotubes

2.5 Optical Properties of Carbon Nanotubes

Carbon nanotubes have unique optical properties. Initially their optical properties received little attention, as photoluminescence is quenched in nanotube bundles by non-radiative relaxation of excited carriers via metallic tubes [9]. This changed since the discovery of direct band-gap photoluminescence from individual tubes in aqueous solutions, enabling direct studies of there optical properties [10]. The 1d confinement of nanotubes affects there optical and electro-optical characteristics. The strong 1d confinement would lead to large columbic coupling between photo excited carrier's electrons (e) and holes (h) to create strongly bound carriers known as excitons. Therefore the absorption and photoluminescence intensity would be enhanced due to the increased e-h overlap. Initial theoretical work indicated that SWNTs had a characteristic electronic structure due to one-dimensional van Hove singularity [11]. Within a zone-folding scheme, one third of all the SWNTs are metallic and two third are semiconducting. The study done by Wilder et al showed that nanotubes of the type n-m = 3a (where 'a' is any positive integer) were metallic and therefore conducting [12]. The fundamental gap would therefore be 0.0 eV. As shown in Fig 2.4 metallic nanotubes have a wider first energy gap between the mirror spikes, whereas the semiconducting nanotubes with the same diameter have small gap. The semiconducting tubes have a fundamental gap which is the function of the diameter, where the gap is of the order of 0.5 eV. At the Fermi energy (highest occupied energy level) the density of states is finite for a metallic tube and zero for a semiconducting tube. As the energy is increased, sharp peaks in the density

of states (van Hove singularities), appear at specific energy levels. Thus the absorption spectra (light as the energy source) should show sharp features at specific energy levels. Depending on the values of chiral vectors n and m of a nanotube, different nanotubes have different transition energies. Optical spectroscopy techniques such as resonant Raman spectroscopy, optical absorption & photoluminescence help probe the direct band-gap of these tubes.
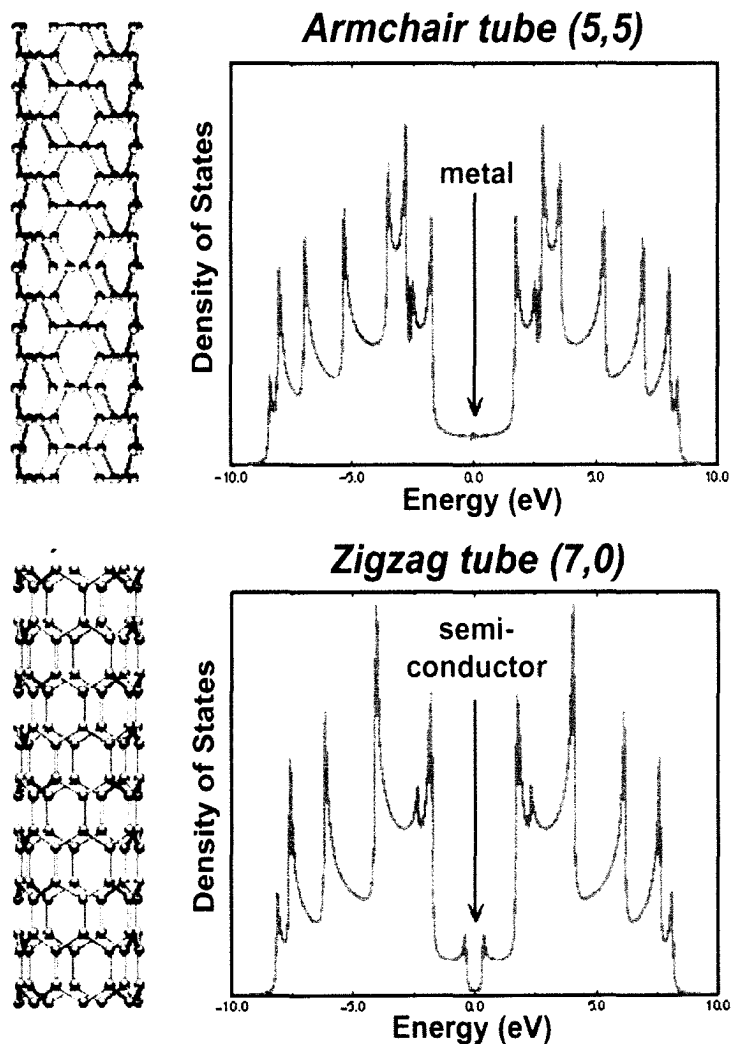
Fig 2.4 Fig density of states of armchair tube and zigzag tube

2.5.1 Resonant Raman spectroscopy of carbon nanotubes

Raman spectroscopy is very useful in understanding the one dimensional properties of carbon nanotubes, since it can probe both the phonon scattering and the electronic structure through the resonant Raman affect [13]. Experimental Raman data on carbon nanotubes confirm earlier theoretical predictions concerning the one-dimensional character of the electronic structure and the density of states. A feature in the 180 – 450 cm^{-1} range of the nanotube Raman spectrum, which is known as the Radial breathing mode (RBM), is diameter selective. According to theoretical predictions, the frequency of the RBM is inversely proportional to the tube diameter [11, 14, and 15]. In the case of an isolated single walled carbon nanotube the RBM can be related to the nanotube diameter with the relation: $\omega_r = 224/d_t$. The RBM Raman band in 180 – 450 cm-1 range is composed of a superposition of single peaks associated with individual nanotubes. Thus the diameter of nanotubes can be obtained from the RBM. The D mode (the disorder mode is located around 1310 cm^{-1}) is expected to be observed in multi walled nanotubes (MWNTs), however when it is seen in semiconducting tubes it is related to the defects in the tubes. The G mode or (TM – Tangential mode) corresponds to the stretching mode in graphite plane. This mode is located around 1580 cm^{-1}. In metallic single walled carbon nanotubes the G-band is usually asymmetric and it fits well with a Breit-Wigner-Fano (BWF) line shape [16, 17 and 18]. The BWF band results from the coupling of the phonons to the electronic continuum of the metallic tubes and is commonly used to distinguish between metallic and semiconducting single walled carbon

nanotubes. For semiconducting single walled carbon nanotubes this band is symmetric in shape. Thus the G-band can be used to distinguish between metallic and semiconducting tubes.

Semiconducting tubes   **Metallic tubes**

RBM   G-BAND   RBM   G-BAND
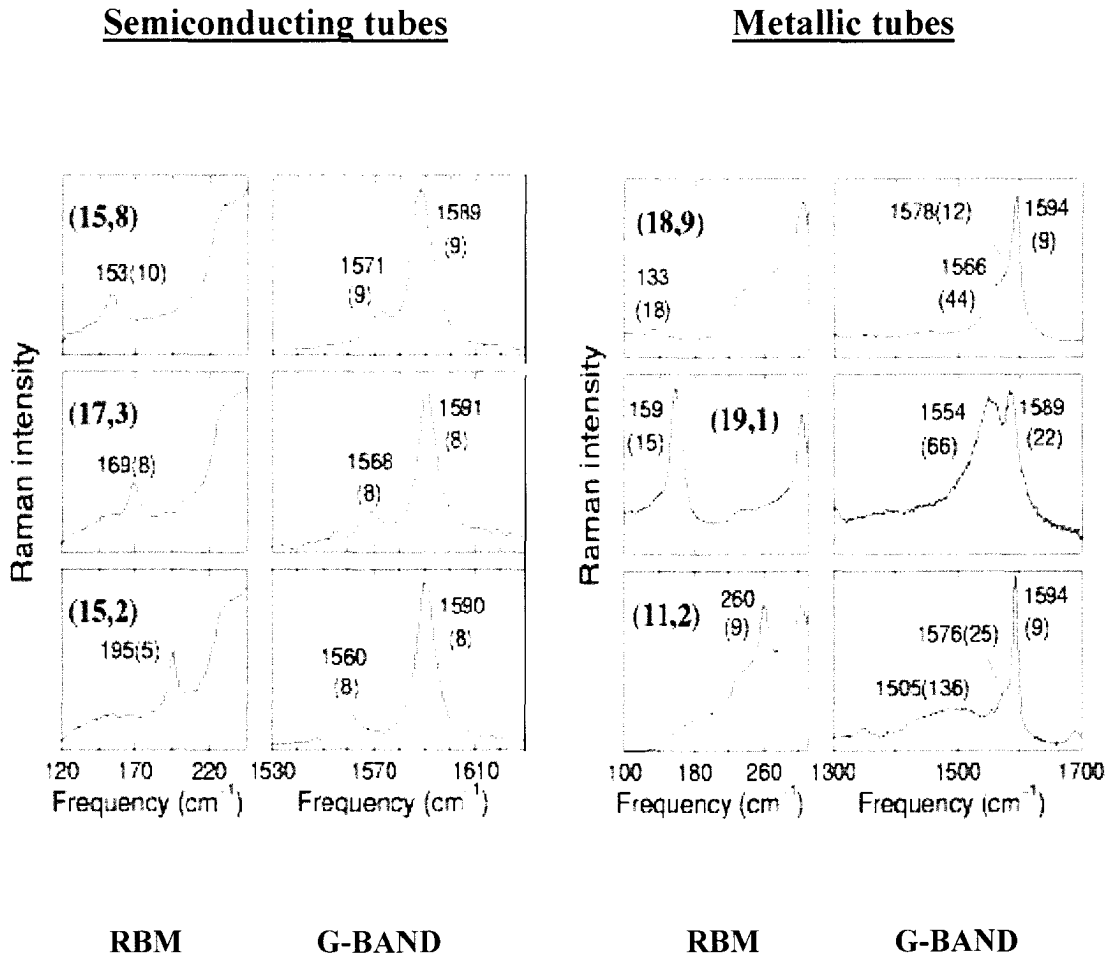
Fig 2.5 Raman spectra of semiconducting and metallic tubes (RBM and G Band)

Fig 2.5 shows the RBM and G-band structure of different chiral vector nanotubes (A.Jario et al). As seen in the figure, the G band data of both semiconducting and metallic tube shows a significant difference. The asymmetric peak in the G band

of the metallic tube is attributed to the Breit-Wigner-Fano (BWF) band, whereas the G band of the semiconducting tube is perfectly symmetric. Radial breathing modes help determine the diameter of the tubes and thus the chiral indices (Kataura Plot).

2.5.2 Optical Light Absorbance of Carbon Nanotubes

Optical absorption is an evaluation method for monitoring the nanotube diameter. Theory predicts that the electronic structure of a single walled carbon nanotube (semiconducting and metallic) depends on the diameter and chiral wrapping angle describing its structure from a 2D graphene sheet [11]. As shown in the Fig 2.6
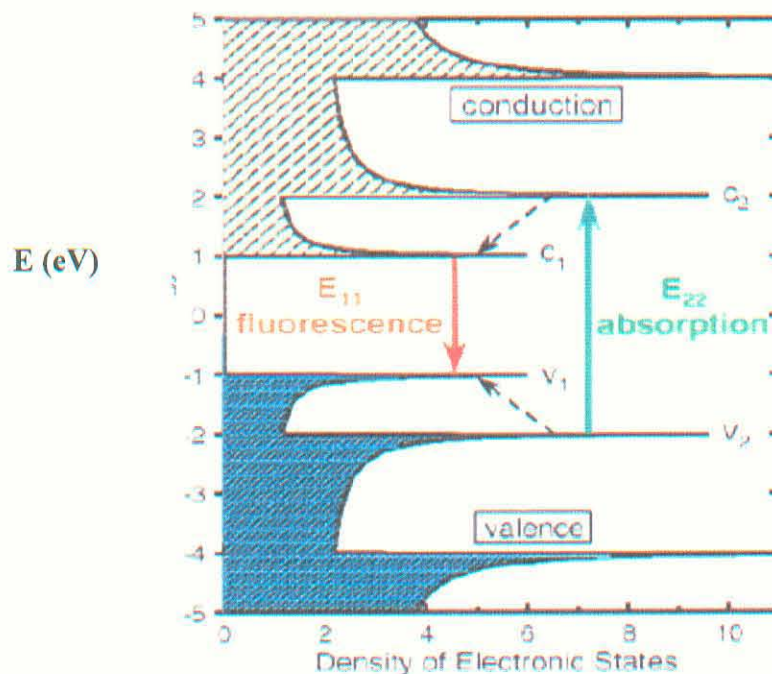
Fig 2.6 Schematic of density of electronic states for single nanotube structure

Quasi-one dimensionality causes the electronic density of states to have a series of sharp van Hove singularities at energies mainly dependant on the diameter of the

14

particular tube. In the figure the solid arrows (green, red) depict the optical excitation and emission transitions between the first and second van Hove singularities known as E_{11} and E_{22} [19]. The dashed arrow in the conduction band denotes the non-radiative relaxation of electron and the dashed arrow in the valence band denotes the relaxation of the hole before emission. As seen in the Figure 2.6, the absorption of photon energy at E_{22} is followed by fluorescence emission near E_{11}.
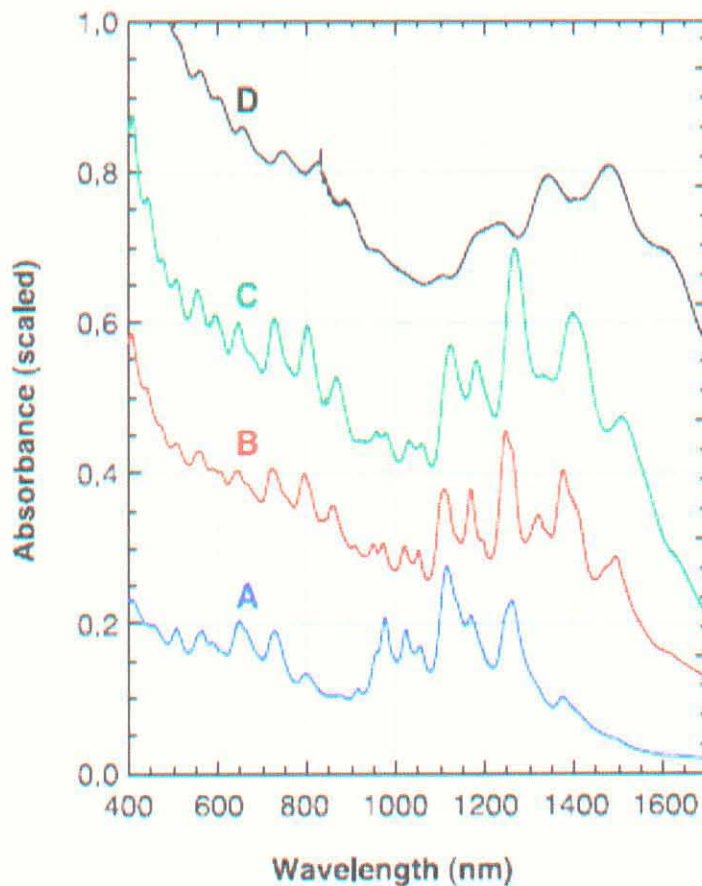
Fig 2.7 Absorption spectra of encapsulant coated SWNT

Fig 2.7 shows the absorption spectra of fullerene nanotubes in SDS-D_2O suspension, done by a group at Rice University (O'Connnell et al). The electronic

absorption spectrum of the solution shows sharp, well structured, narrow width spectral features. Superposition of different electronic transitions from a variety of carbon nanotubes gives rise to these distinct optical spectral features. As seen in Figure 2.7, the electronic absorption spectrum of particular tubes is expected to be dominated by a series of relatively sharp inter-band transitions, at energies E_{11}, E_{22} etc associated with van Hove singularities [10]. For the semiconducting tubes, the first van Hove transition; E_{11} falls in the 800 – 1600 nm range, the second van Hove transition is in the 550 – 900 nm range and the lowest energy van Hove transitions of the metallic tubes appear between 400 – 600 nm. The absorption spectra above shows four traces, different diameter nanotubes that were individually dispersed (traces A, B & C) and un-separated nanotube bundles in liquid solution (trace D).

2.5.3 Optical light emission from carbon nanotubes

Two-thirds of the nanotubes are predicted to be direct band gap semiconductors; thus photoluminescence from the recombination of electrons and holes is expected at the band-gap [20]. The ability of a material to luminesce depends on its intrinsic band structure and also on other internal and external factors. Examples of internal factors are surface reconstructions, surface or bulk defect states and dopants. Examples of external factors are the dielectric environment, electric and magnetic fields and external chemical reactions. These factors can fill or deplete the bands and change the entire band structure, thus the photoluminescence intensity can be affected. Since carbon nanotubes have all the constituent atoms on the surface, they are directly exposed to their surroundings,

which in turn can influence their optical properties. Photoluminescence is a direct optical probe of the electronic band structure of SWNTs.

The biggest obstacle in studying the optical properties of carbon nanotubes is aggregation of tubes [21]. Aggregation causes bundling, which perturbs the electronic structure of the tubes and makes it difficult to study their optical properties. These small bundles of tubes have (non-luminescent) metallic tubes which quench the electronic excitation on an adjacent semiconducting tube, preventing luminescence.
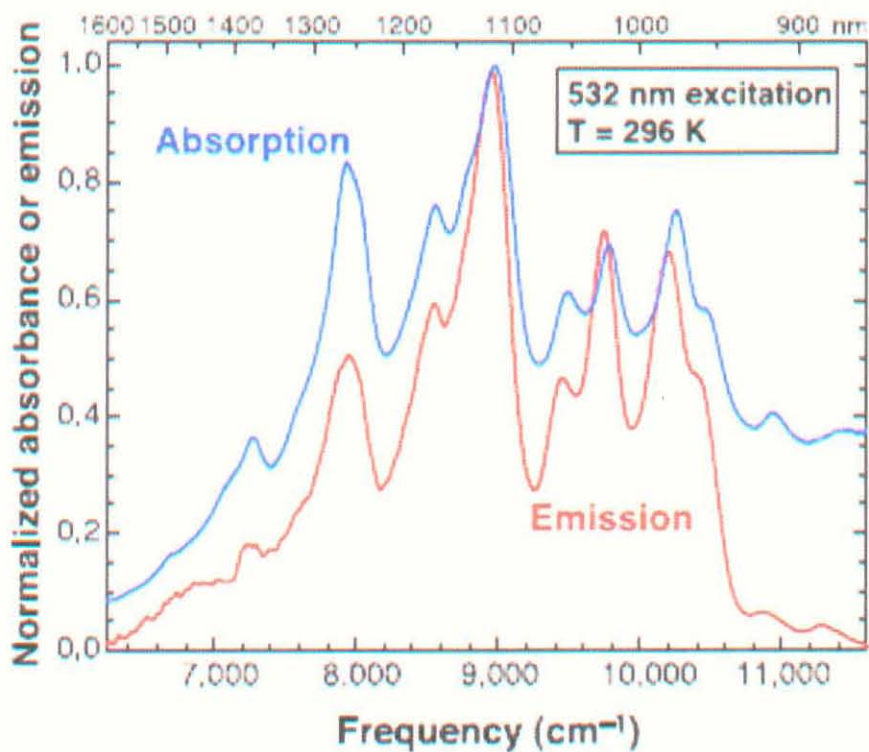
Fig 2.8 Absorption and emission spectra of individual carbon nanotubes suspended in SDS micelles in D$_2$O suspension

Band gap fluorescence from individual single walled carbon nanotubes was first demonstrated by a group at Rice University (O'Connell et al). They developed a

method in which individual carbon nanotubes were encapsulated in cylindrical micelles, by ultrasonically agitating an aqueous dispersion of SWNTs in sodium do-decyl sulphate and then centrifuging to remove tube bundles, ropes, and residual catalyst. As shown in Figure 2.8, the suspension of this encapsulant wrapped single walled carbon nanotubes displayed bright, structured photoluminescence in the near infrared. The figure shows a comparison of the excitation and emission spectra. Each absorption component in the spectral region of first van Hove transition is present in the emission spectrum, making it possible to assign the emission to semiconducting tubes. Bright, well structured emission in the near infra red confirmed that no aggregation of tubes took place in the sample. As explained earlier, optical excitation of a semiconducting tube in its second van Hove transition, E_{22}, is followed by rapid electronic relaxation before emission in the first transition, E_{11}.

2.6 Electrical Properties of Carbon Nanotubes

One promising direction for the transistors of the future is "molecular electronics" in which the active part of the device is composed of a single or a few molecules. The most widely studied form of molecular electronics is based on carbon nanotubes [22] [23]. The small diameter and the long length of single-walled carbon nanotubes lead to very large aspect ratios that make them almost ideal one – dimensional systems which in turn imply reduced carrier scattering and the possibility of ballistic devices. Also the chemical bonds in nanotubes are very strong leading to extremely high mechanical, thermal and chemical stability.

The unique electrical properties of SWNTs arise from the confinement of the electrons in the carbon nanotubes. This allows for motion in only two directions along the tube axis: forward and backward. Along with the requirements for energy and momentum conservation this leads to a reduced "phase space" for the scattering processes that establishes the minimum electrical resistance of the carbon nanotubes [22] [23] [24]. To measure the electrical properties of SWNTs, they are connected to metal electrodes produced by lithographic techniques
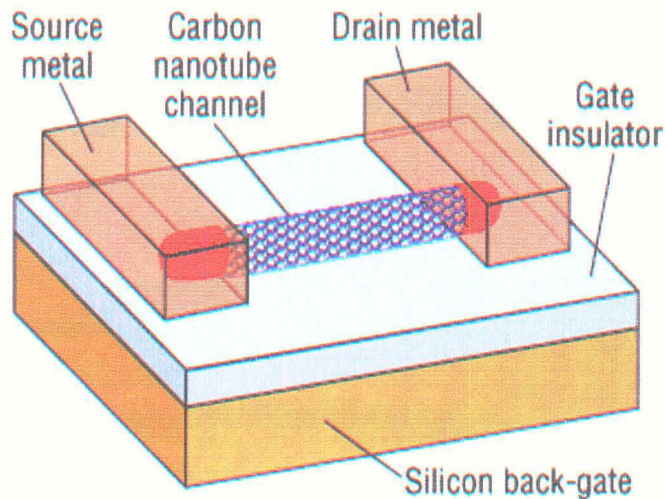
Figure 2.9 Schematic of a CNTFET device

The first field effect transistor using the carbon nanotubes was fabricated in 1998 [25] [26]. The structure of these carbon nanotube field effect transistors (CNT-FETs) is very simple; a single-walled carbon nanotube was positioned to bridge two metal electrodes, which acted as both source and drain of the CNT-FET. The

electrodes are fabricated on top of an oxidized silicon wafer the (heavily doped) wafer itself was used as the gate electrode. These CNT-FETs behaved as p-type FETs, as the dominant carriers were holes. The ON/OFF current ratio was measured to be around 10^5. Although functional, these devices had a parasitic resistance greater than 1MΩ, low drive currents and a low trans-conductance. As shown in Figure 2.10 (a) shows the output characteristics of (Ids vs. Vds) for a 600 nm long, 1.8 nm diameter, back gated CNT-FET. Figure 2.10 (b) shows the transfer characteristics of a large diameter tube (1.8 nm) at different drain voltages.
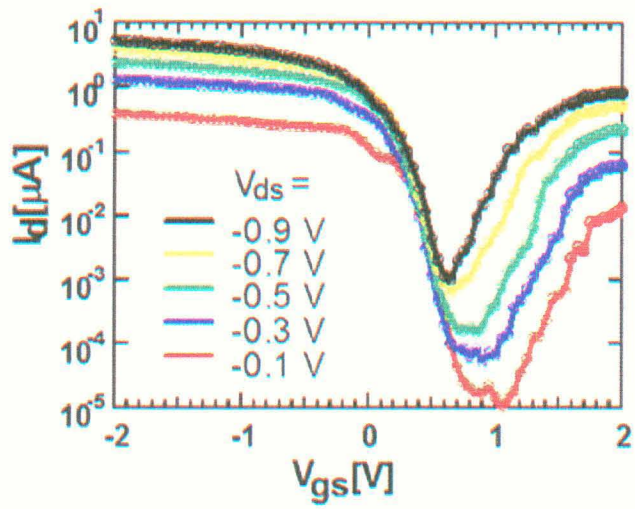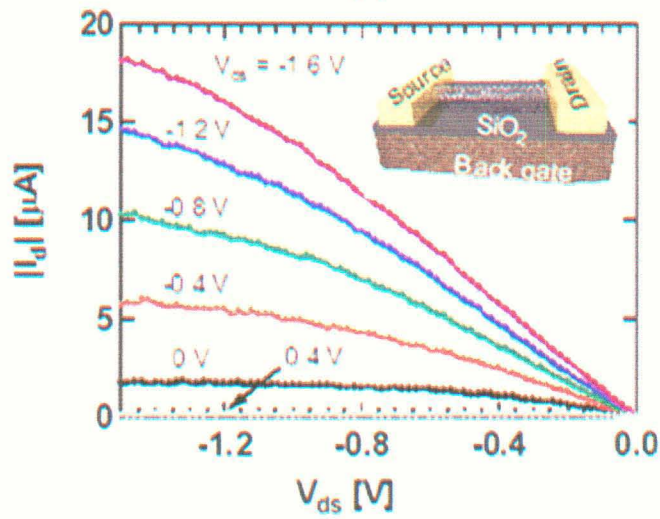
Fig 2.10 (a) Output characteristics (I_{ds} vs. V_{ds}) of a back gated CNTFET,
(b) Transfer characteristics of large diameter CNTFET

CHAPTER III

SWNT$_S$ SAMPLE PREPARATION & SPECTROSCOPY MEASUREMENTS

A major obstacle to the study of nanotube optical properties is the separation of tubes with different diameter and chiral angles. Photoluminescence of carbon nanotubes is quenched if they are aggregated together in bundles; also, the tubes that contact the substrate do not luminescence. To study the optical properties of individual carbon nanotubes, they must be detached from the bundles by physical means, bundles of tubes must be removed and the individual tubes must be suspended in a stable environment or nanotubes should be grown in a way that they are not in physical contact with the substrate. Two methods have been reported which help study the optical properties of individual carbon nanotubes.

3.1 Sample preparation

(a) Suspending carbon nanotubes in liquid solution: In this method carbon nanotubes are wrapped with different encapsulants (using vigorous sonication treatment followed by ultra centrifugation), thus preventing re-aggregation of tubes [10].

(b) Direct growth of individual nanotubes suspended in air between pillars: Carbon nanotubes are grown directly by chemical vapor deposition method (CVD) atop pillar arrays on patterned silicon arrays [20].

In this thesis, method **(a) "suspending carbon nanotubes in liquid solution"** was used.

The recipe used for this process is as follows:

Recipe:

(a) Raw carbon nanotubes were dispersed in 100 ml of aqueous SDS (1 % weight) solution.

(b) The dispersion was then treated in a cup-horn sonicator (Cole Parmer 750 W CPX) for 10 minutes at 50 % amplitude of maximum power.

(c) The sonicated sample was immediately centrifuged (Beckman ultracentrifuge with surespin 630 swing bucket rotor) at 70,000 g for four hours.

(d) The upper 75 to 80 % supernatant was carefully decanted.

The above mentioned recipe was used for encapsulating commercially purchased nanotubes: HiPCO (High pressure carbon monoxide reactor) purchased from Carbon Nanotechnologies Inc and CoMoCAT (Cobalt molybdenum catalyst) from Southwest Nanotechnologies Inc. The sonication and ultracentrifuge process helps break bundles of carbon nanotubes, separate them, and wrap them with different encapsulants and separate individual encapsulated tubes from small bundles and residual catalyst particles.

3.1.1 Sonication process:

Bundles of carbon nanotubes are bound together by van der Waals energy (~ 500 eV per micrometer of tube-tube contact) which holds them together. The

sonication process helps break these van der Waals forces and separates the tubes. The surfactant in the aqueous solution adsorbs on the surface of these separated tubes which prevents the aggregation or re-bundling of tubes. High power sonication treatment to these tubes also leads to inter-tube cutting. However, the optical spectra of these samples, including the strong RBM (Radial breathing mode) in $150 - 400$ cm^{-1} range in the Raman spectra and the near absence of the "disorder peak" at around 1300 cm^{-1} strongly suggest that the high power sonication treatment did not substantially damage the tube or tube side walls.

3.1.2 Centrifuge process:

The centrifuge process, performed immediately after sonication exploits the differences in buoyant densities (mass per volume) among SWNTs of different structures, bundles and impurities. Nanotube bundles, residual catalyst particles and impurities having higher buoyant density compared to individual tubes are settled at the bottom of the centrifuge tube, leaving a supernatant which is highly enriched in micelle encapsulated single walled carbon nanotubes. Typical samples contain 3-5 nm catalyst particles, each coated with 1 or 2 atomic layers of carbon. In SDS micelles, these residual catalyst particles have a density near 2 to 3 g/cm^3. A method known as 'density gradient differentiation (DGU)' was recently reported for sorting carbon nanotubes by electronic structure. Carbon nanotubes were separated by diameter, band-gap and (metallic or semiconducting) electronic type using DGU.

3.1.3 Encapsulant adsorption on nanotube surface:

The encapsulants used for the separation of nanotubes have (a) hydrophilic head and (b) hydrophobic tail. Carbon nanotubes are hydrophobic in nature. Encapsulant adsorption on the nanotube can be considered a two step process: (1) "Head to tail" parallel to the nanotube surface: the hydrophilic head of the encapsulant molecule adsorbs on the nanotube surface and forms a compact outer surface, protecting the nanotube from water molecules. (2) "Tails on" flat surface: as the surface coverage increases due to the encapsulant adsorption parallel to the nanotube surface and forms a monolayer, the hydrophobic tails of encapsulant molecules stand up in a "tails on" configuration until the adsorption reaches equilibrium [28]. Thus nanotubes are preserved in a pure hydrocarbon environment. The hydrophobic tails of the encapsulants can adopt a wide range of orientations with respect to the tube. These encapsulant molecules are long and they can bend and even turn around to wrap the nanotube surface. These molecules are polar, thus due to Columbic repulsions between 'like' charged molecules aggregation of nanotubes is prevented. Water molecules have a small probability to penetrate into the hydrophobic tails, reaching close to the center of hydrocarbon environment. However, water molecules do not reach in the direct vicinity of tubes, so individual tubes are preserved in a pure hydrocarbon environment. The encapsulant molecules lie along the nanotube surface, the molecules parallel to the surface tend to adsorb well compared to the molecules across the nanotube axis. Figure 3.1 (a) shows an individual fullerene nanotube encapsulated in a SDS micelle and Figure 3.1 (b) shows a seven-tube bundle

coated with SDS micelle. The individual nanotube encapsulated SDS micelle has a specific gravity of 1.0 g/cm^3 and that of the seven- tube bundle is 1.2 g/cm^3 [10].

(a)   (b)
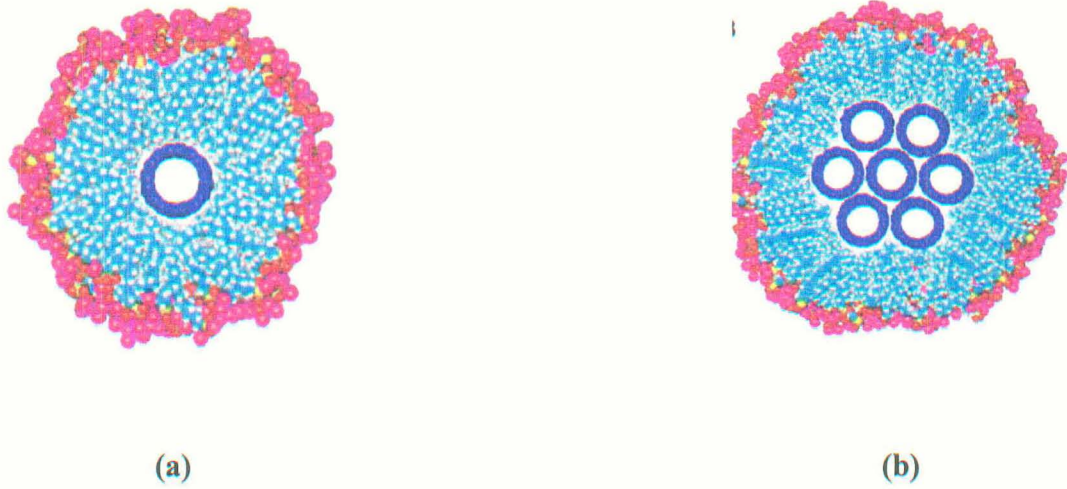
Fig 3.1 (a) Individual fullerene nanotube in a cylindrical SDS micelle

(b) Seven tube bundle of nanotubes coated by a layer of SDS

Encapsulants used:	Nanotubes:	Experiments:
(a) SDS (Sodium Do-decyl Sulphate)	HiPCO (High pressure carbon monoxide)	Absorbance, ph dependence, photoluminescence
(b) Pluronic F-108	HiPCO	Absorbance, photoluminescence
(c) Sodium Cholate (SC)	CoMoCAT (Cobalt molybdenum catalyst)	Absorbance, photoluminescence
(d) DNA	CoMoCAT	Absorbance, photoluminescence
(e) Na-CMC (Sodium Carboxy-methyl-cellulose)	CoMoCAT	Absorbance, photoluminescence

Table 1: Various encapsulants used for wrapping single walled carbon nanotubes

3.2 Optical characterization:

3.2.1 Raman Spectroscopy:

Raman measurements were performed on thin films of carbon nanotubes encapsulated in Na-CMC. The excitation wavelength was 632.8 nm (1.92 eV).
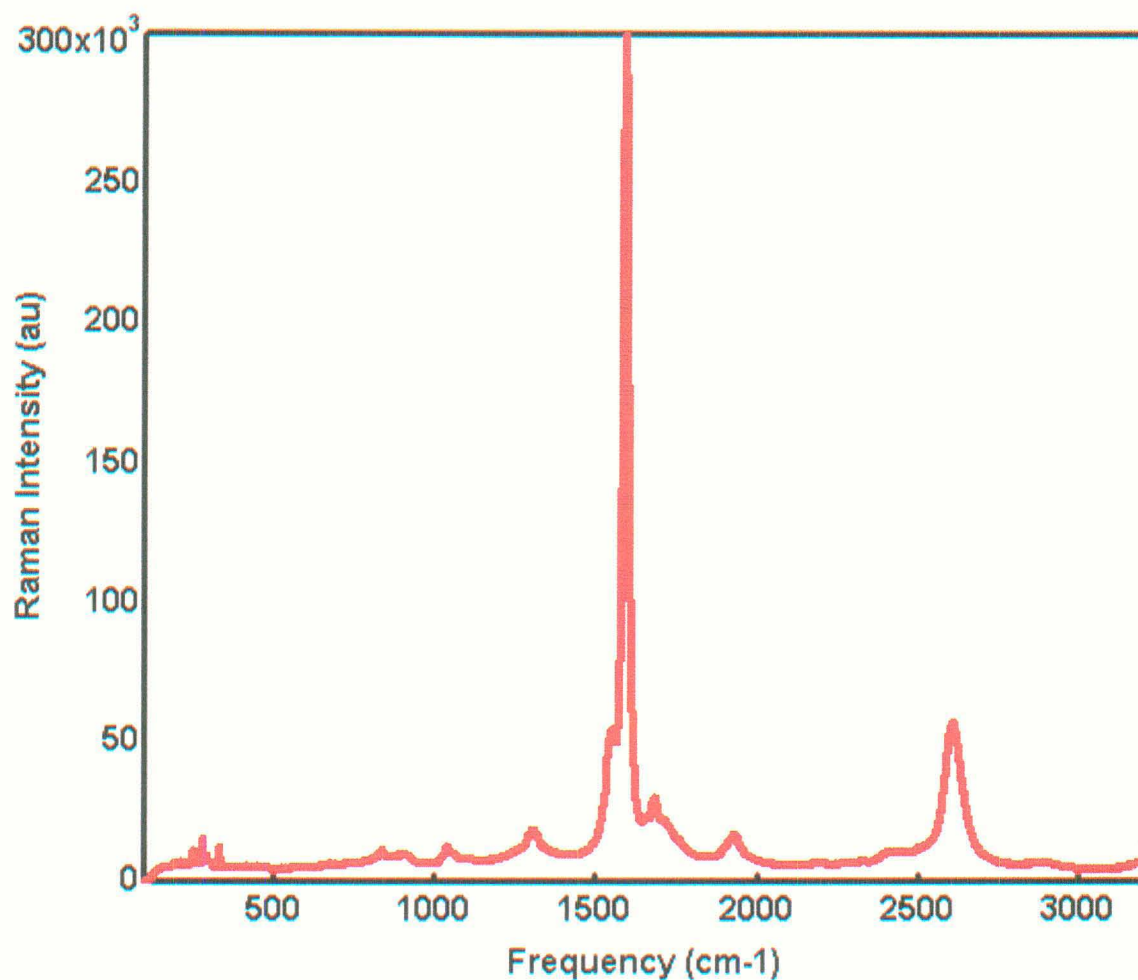
Fig 3.2 Raman spectra of single walled carbon nanotubes

Raman measurements show the RBM (Radial breathing mode) in 180-400 cm^{-1} range, D mode (the disorder band) which is located around 1300 cm^{-1} and the G mode (tangential mode) located around 1580 cm^{-1}.
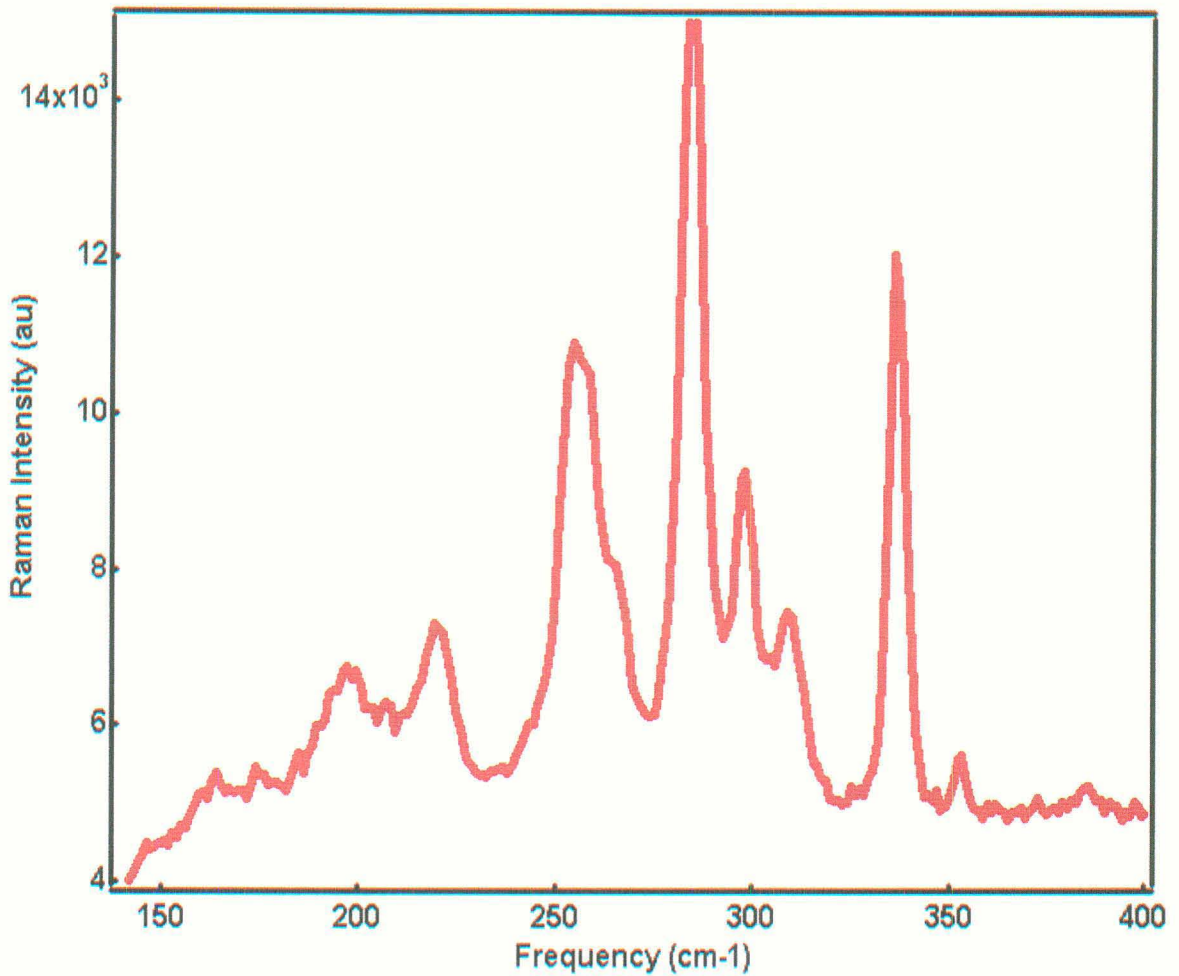
Fig 3.3 Raman spectra of the radial breathing mode (RBM) of SWNTs

Figure 3.3 shows the Raman spectra of radial breathing mode (RBM) of single walled carbon nanotubes at a single excitation wavelength (1.92 eV). As mentioned earlier, according to theoretical predictions, the frequency (Raman shift) of the RBM is inversely proportional to the tube diameter [11, 14 and 15]. In the case of an isolated single walled carbon nanotube the RBM can be related to the nanotube diameter with the relation: $\omega_r = 224/d_t$, where ω_r is the RBM frequency, d_t is nanotube diameter. Using this relation the diameters for

CoMoCAT tubes were found to be between 0.66 – 1.021 nm. The average diameter was calculated to be approximately 0.80 nm. The diameter range for CoMoCAT carbon nanotubes matches with the diameter range predicted by other groups [29]. The chiral indices (n, m) of different diameter tubes were obtained using a Kataura plot [16].

Raman Shift (cm-1)	Diameter (nm)	Chiral indices (n, m)
219.27	1.021	(12, 3)
254.44	0.88	(11, 1)
285.07	0.78	(6, 5)
295.15	0.75	(8, 3)
309.15	0.72	(7, 4)
336.16	0.66	(6, 4)

Table 2 shows the Raman shift, diameter and chiral vectors (n, m) of SWNTs
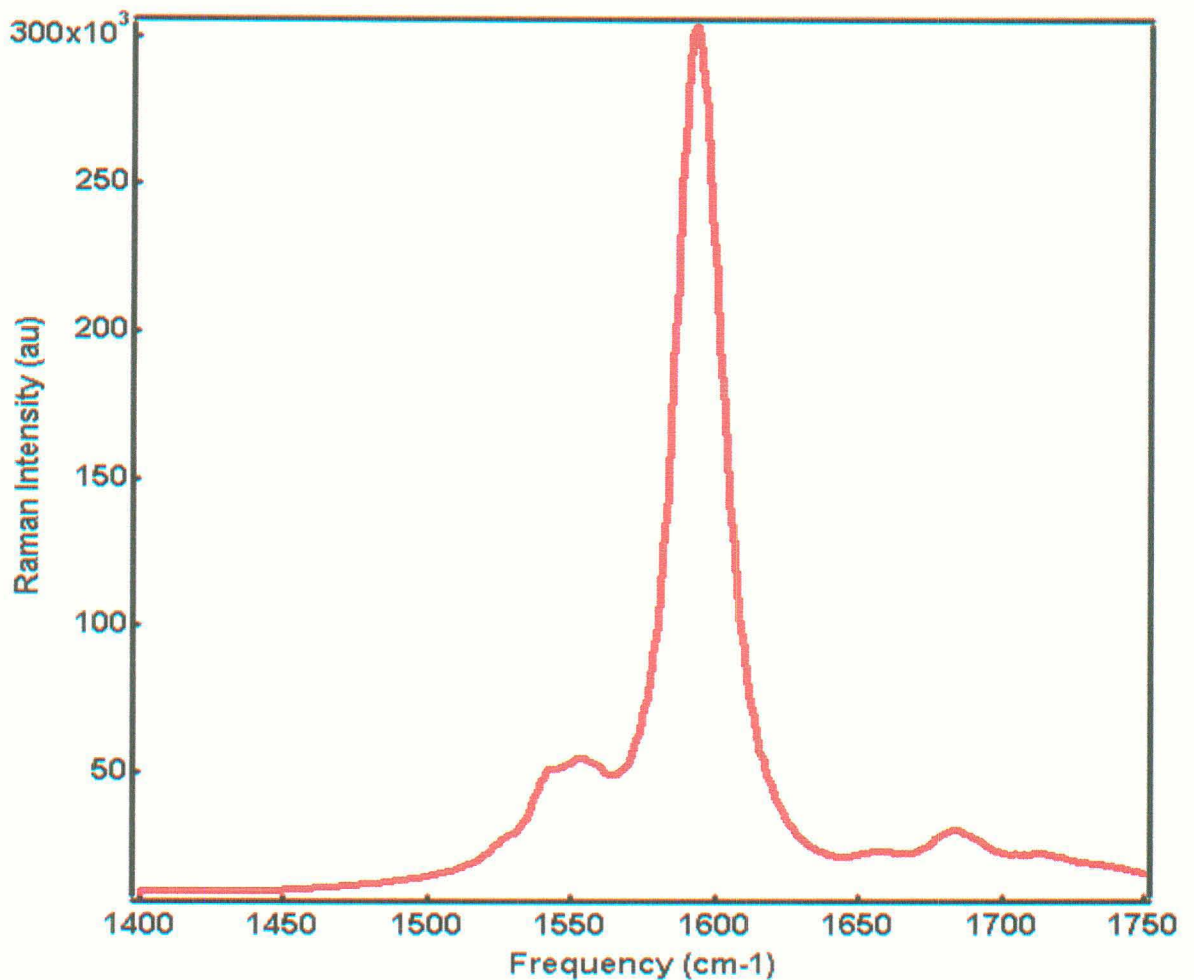
Figure 3.4 Raman spectra of the G mode (TM – Tangential mode) of

SWNTs

Figure 3.4 shows the Raman spectra of G mode of SWNTs at 1592.8 cm^{-1}. The G

mode corresponds to the stretching mode in the graphite plane; it is a sum of high-

energy tangential modes that originate from breaking the symmetry of tangential

vibration when the graphene sheet is rolled into a tube. The line shape of the G

mode distinguishes the semiconducting and metallic tubes. The G feature is

broadened and asymmetric for metallic SWNTs and is usually fit using Breit-

Wigner-Fano (BWF) line, as shown in Figure 2.6 for metallic tubes [16, 17 and

18]. The G band for semiconducting tubes is symmetric, usually a lorentzian line

shape, thus the observed G band, suggested that most of the tubes were semiconducting, with fewer metallic tubes in number.

3.2.2 Optical absorbance and photoluminescence spectroscopy:

(a) SDS (Sodium do-decyl sulphate) encapsulated HiPCO SWNTs:

Absorbance and photoluminescence measurements were carried out on SDS (Sodium do-decyl) encapsulated HiPCO (High pressure carbon monoxide reactor) single walled carbon nanotubes.
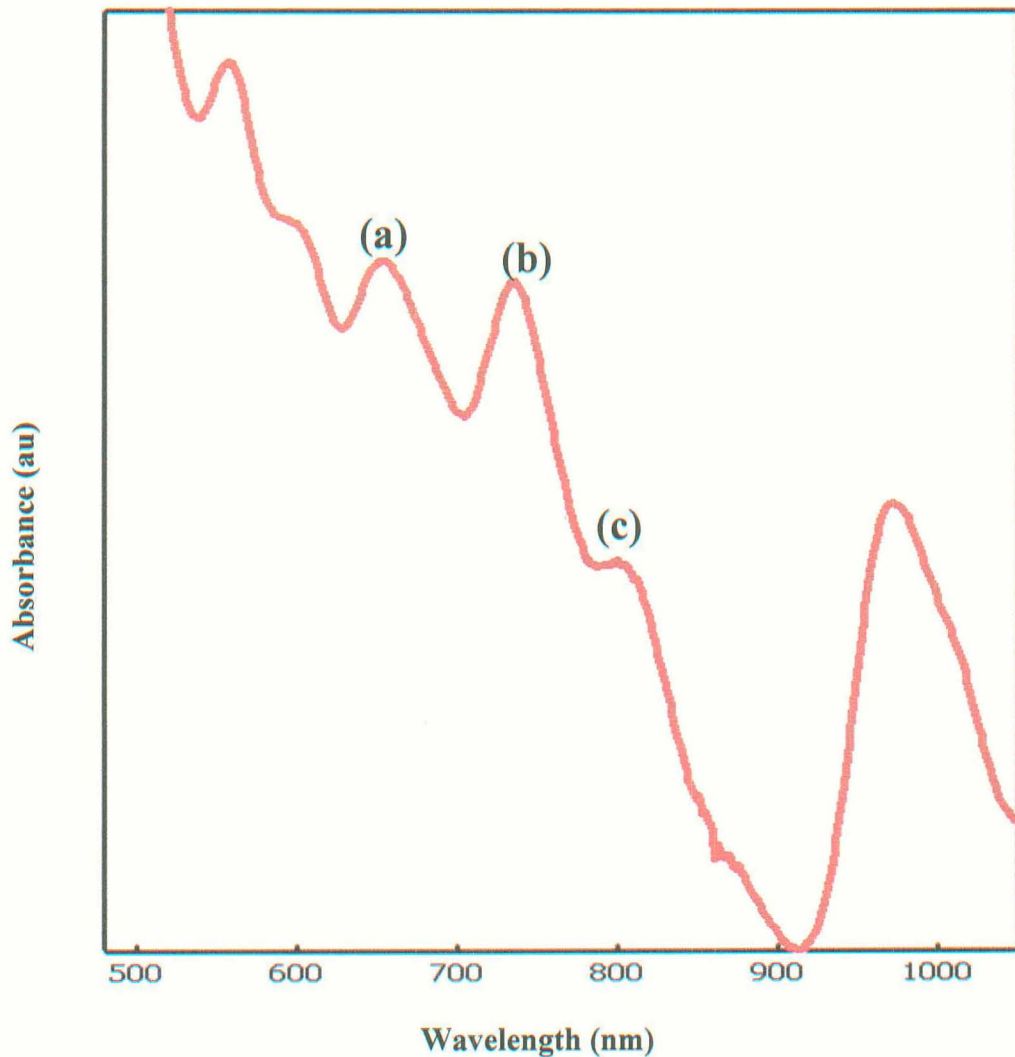
Fig 3.5 Absorbance spectra of SDS/HiPCO single walled carbon nanotubes

The measurements were performed in an Ultraviolet-Visible-Infrared Spectrometer (Perkin Elmer λ 950). Figure 3.5 shows the absorbance spectra of SDS encapsulated HiPCO single walled carbon nanotubes. Narrow, sharp, well structured, symmetric optical features were obtained in the visible and near infra red spectrum. These spectral features are a superposition of distinct electronic transitions from a variety of fullerene nanotubes isolated within the SDS micelles. As discussed in section 2.5.2, the optical light absorption spectrum of carbon nanotubes is dominated by a series of relatively sharp inter-band transitions at energies associated with transitions between the van Hove singularities [19]. As seen in the Figure 3.5 the first van Hove transition E_{11} falls in the 800 – 1100 nm range, and the second van Hove transition E_{22} (with a slight overlap in the first transition) lies in the 550-900 range. The energy separation of a particular carbon nanotube can be obtained from the distinct absorbance peaks. The energy separation of the absorbance peak observed at (a) 653 nm is 1.90 eV, (b) 735 nm is 1.68 eV and (c) 804 nm is 1.54 eV. Using this energy separation in the particular transition regime [(E11 800 – 1100 nm) or (E_{22} 550 – 900 nm)] the approximate (n, m) chiral indices for these tubes using Kataura plot [16] were calculated. Figure 3.6 shows the Kataura plot used to assign the chiral indices (n, m) to these tubes. Kataura plot shows the energy separation vs. the diameter distribution for various transitions (E_{11}, E_{22} or M_{11}) for semiconducting and metallic tubes. As seen in the figure the first distribution is E_{11}, the second E_{22}, third is M_{11} and so on for higher energy transitions. The black line represents the semiconducting tubes and the red line shows the transition for metallic tubes.
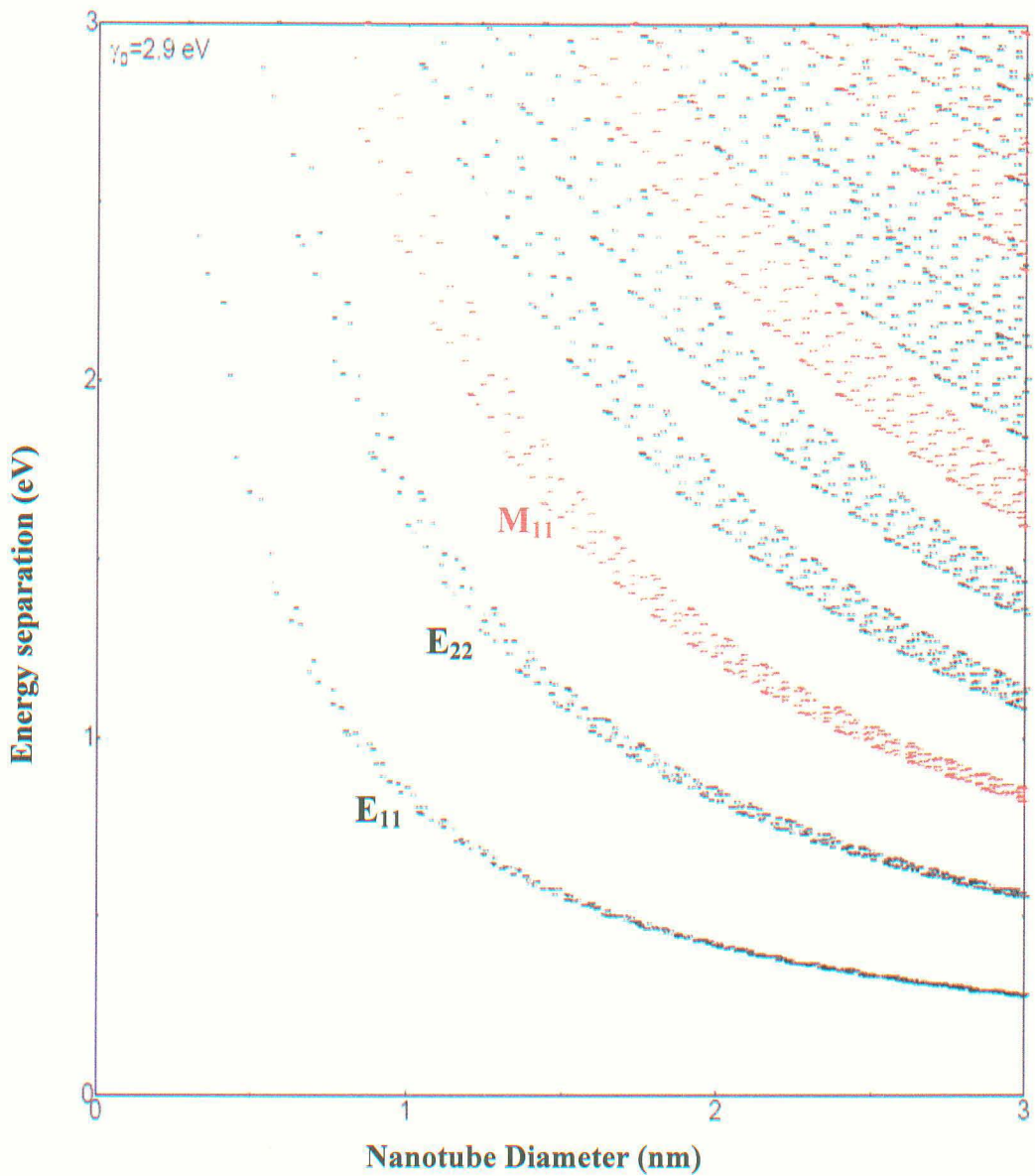
Fig 3.6 Kataura plot of Energy spacing vs. nanotube diameter distribution

With a fixed diameter range for this sample (0.65 – 1.2 nm) and the energy separation for three different peaks, there approximate chiral indices as calculated; (a) peak at 653 nm, energy separation 1.90 eV, chiral index (n, m) is (7, 5) (b) peak at 735 nm, energy separation 1.68 eV, chiral index is (8, 7) and (c) peak at 804 nm, energy separation 1.54 eV, chiral index is (12, 5).

It was observed in the absorbance spectra that acidic solutions with pH < 7 display broad, unstructured features. However, a well structured spectrum was observed when the solution was neutralized to pH > 7. Figure 3.7 shows the comparison of the absorption spectrum of two solutions with pH = 6 (red line) &

pH = 6, Red line
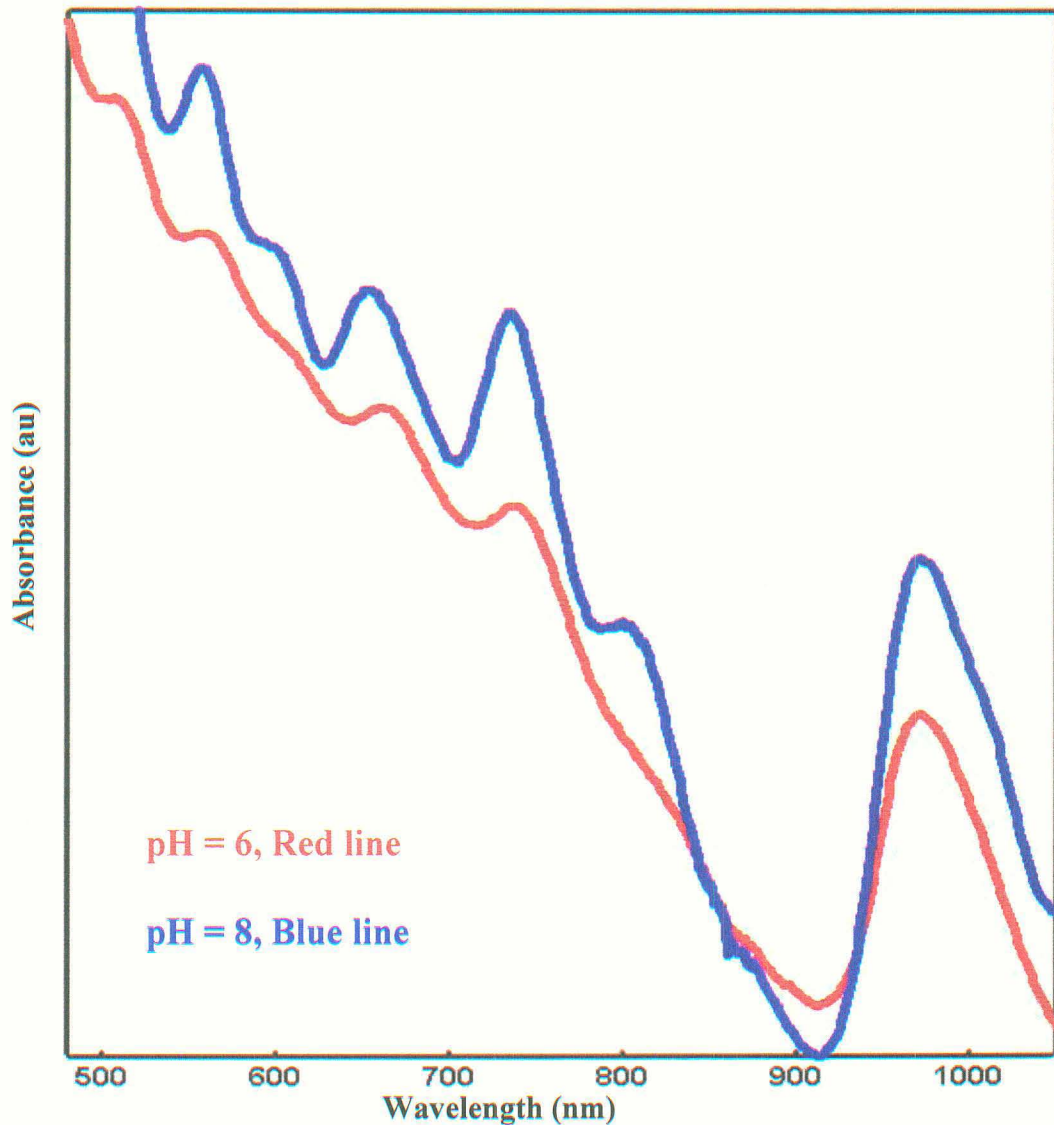
pH = 8, Blue line

Fig 3.7 Absorption spectra of alkaline and non-alkaline SDS/HiPCO carbon nanotubes solution

and pH = 8 (blue line)This process can be explained as electron transfer mechanism [30]. To change the pH value of the solution to 8, 24 % w/v NaOH was added. Addition of sodium hydroxide introduces electron donor sites in the sample. This addition of electron donor sites increases the transition strength of the carriers within the same regime, thus well defined, sharp spectral features are observed on increasing the pH value. Similarly if the pH values were decreased below 3, by introducing electron acceptor sites (e.g. HCl), it would result in a decrease in the transition strength of the carriers and thus the spectral features would be very small or almost disappear.
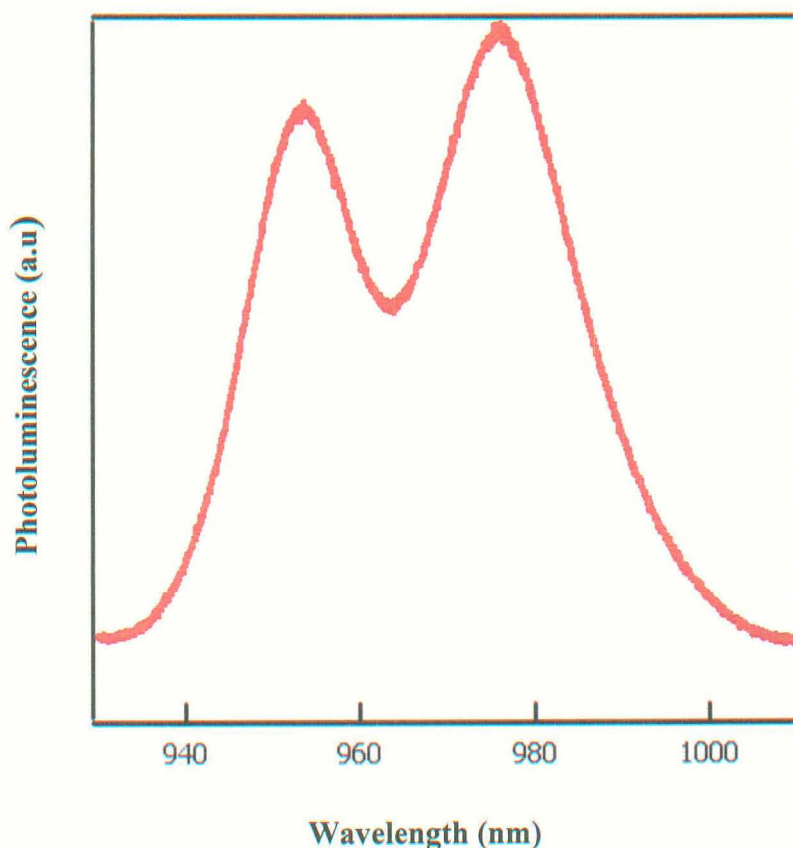
Fig 3.8 Photoluminescence spectra of SDS/HiPCO carbon nanotubes

As shown in Figure 3.8 bright photoluminescence in the infrared range was observed from SDS encapsulated HiPCO carbon nanotube solution. It was observed that photoluminescence intensity drastically reduced upon aggregation of individual tubes by acidification of the sample. Narrow, sharp, well structured features were obtained in the emission spectrum of this solution. Two sharp peaks were obtained at 957 nm and 979 nm. From the energy separation, the peak at 979 nm (1.26 eV) is the E_{11} transition of the (6, 5) tube and the peak at 957 nm (1.29 eV) corresponds to the E_{11} transition of (8, 3) tube. However, comparing the photoluminescence data with the absorbance data, there was no corresponding overlap as seen by other groups [10]. The two sharp, well structured features in the emission spectrum suggest that they might not have been resolved in the absorption spectrum; however it could even be an optical alignment issue.

(b) Pluronic F-108 encapsulated HiPCO SWNTs:

Pluronic F-108 is a water soluble, bio-compatible polymer of the Pluronic series. It is a PEO-PBO-PEO triblock polymer, stabilized by PEO chains. It is a higher molecular weight (14, 600 U) polymer, which enhances the suspend-ability of carbon nanotubes. As the PEO chains of the Pluronic polymer extends into water, they impede nanotube aggregation, which is different compared to SDS (sodium do-decyl sulphate) where aggregation was prevented due to similar charge repulsion from hydrophobic tails [31]. Pluronic F-108 being a bio-compatible polymer, carbon nanotubes coated with F-108 were exposed to live cells and the

life time of these cells was studied [32]. This polymer could be used for studying the effect of carbon nanotubes on several biological agents.
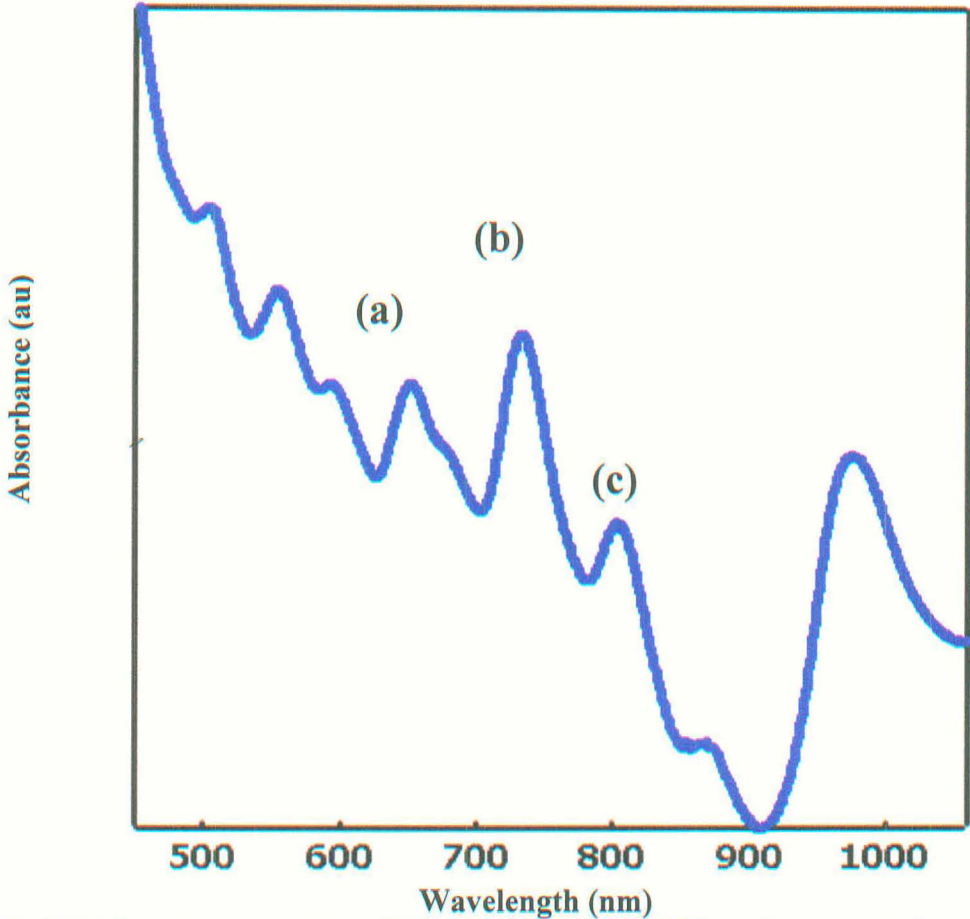
Fig 3.9 Absorbance spectra of Pluronic F-108/HiPCO carbon nanotubes

Figure 3.9 shows the absorbance spectra of Pluronic F-108 encapsulated HiPCO single walled carbon nanotubes. As observed in the absorbance spectra of SDS encapsulated tubes, the absorbance spectra for Pluronic F-108 encapsulated tubes showed excellent sharp, narrow, well structured optical features, representing a superposition of electronic transitions from a variety of fullerene nantoubes. Comparison of the absorbance data of SDS and Pluronic F-108 encapsulated single walled carbon nanotubes showed a striking resemblance. No significant

peak shifts were observed between the two data sets. As discussed for SDS encapsulated tubes the energy spacing for the peaks at (a), (b) and (c), was found to be 1.90 eV, 1.69 eV and 1.54 eV respectively. Thus no significant peak shift was observed for Pluronic F-108 encapsulated tubes when compared with SDS encapsulated tubes. The chiral indices for the three observed peaks were the same as that observed for SDS encapsulated tubes; (a) (7, 5) (b) (8, 7) (c) (12, 5).
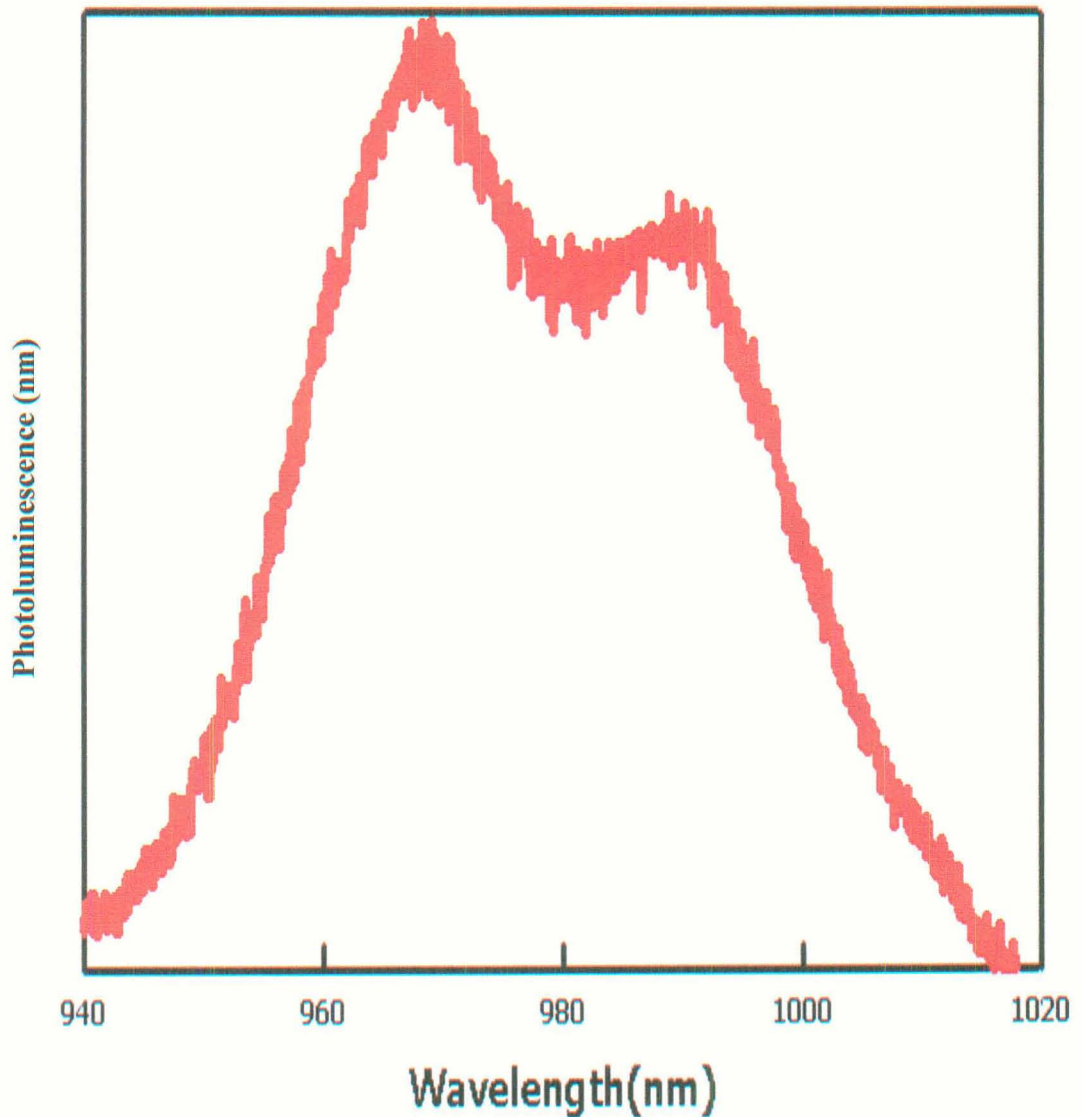
Fig 3.10 Photoluminescence spectra of Pluronic F-108/HiPCO SWNTs

Two peaks were observed in the near infra red range. The excitation wavelength was 488 nm (2.54 eV).The optical emission features were broad and asymmetric in shape. This could be because of fewer tubes being encapsulated with Pluronic F-108 or significant damage of micelle structures. The two peaks were observed at 965 nm and 990 nm. Comparing the peak positions with SDS encapsulated nanotubes emission spectra (fig 3.8), we find that the peaks were slightly shifted. This could be attributed to the different encapsulants used. Other groups have predicted this peak shift [31]. As observed in SDS encapsulated tubes, the photoluminescence peaks did not show a striking correspondence with the absorption spectra of Pluronic F-108 (Fig 3.9) encapsulated tubes. As mentioned earlier, this could be due to unresolved peaks in the absorption spectrum or optical alignment issue. However, from the energy spacing and the diameter of the tubes, the chiral indices of these peaks are as: peak at 965 nm is (8, 3) tube and peak at 990 nm is (6, 5) tube.

(c) Sodium Cholate (SC) encapsulated CoMoCAT SWNTs:

Sodium cholate is a natural bile (obtained from ox or sheep) salt detergent. It is a sodium salt of cholic acid. Sodium cholate molecules have alkyl chains as long as 24 carbon atoms. It is worth noting that sodium cholate has an excellent optical transparency, well into the UV (down to ~ 200 nm) [33]. Sodium cholate was found to be an excellent dispersant of single walled carbon nanotubes. Bile salts have a linear and a very flexible apolar tail, the more apolar half of the bile salt molecule consists of a semi-rigid cholesterol group which usually possesses both

a hydrophobic and a hydrophilic face [34]. The flattened bean shape of this group is particularly suitable for stacking into ordered layers, hence the interaction energy between neighboring surfactant molecules is at least as important as the surfactant-SWNT interaction. The strong tendency of cholesterol derivatives to organize into ordered layers is exemplified by the fact that cholesterol is also a well-known building block for many chiral liquid crystals [35]. Bile salt molecules can diffuse rapidly and quickly cover a nanotube surface as soon as they are exposed (either by thermal or by mechanical agitation), thus a very stable and ordered cylindrical layer could be readily formed around carbon nanotube templates [33]. Thus sodium cholate was used to encapsulate CoMoCAT (Cobalt molybdenum catalyst) carbon nanotubes, which are enriched with (6, 5) tubes.

Fig 3.11 Absorbance spectra of SC/CoMoCAT SWNTs

Figure 3.11 shows the absorption spectrum of sodium cholate encapsulated single walled carbon nanotubes. Excellent sharp, narrow, symmetric optical features were obtained in the absorbance spectra. Two sharp peaks were obtained at (a) 573 nm and (b) 988 nm. The energy spacing of these peaks was (a) 2.16 eV and (b) 1.25 eV. Using the Kataura plot the chiral indices of the tubes which show this peak were calculated. It was observed that the peak at 990 nm (1.25 eV) corresponds to the E11 transition of (6, 5) tube and the peak at 573 nm (2.16 eV) corresponds to the E22 transition of the same (6, 5) tube.

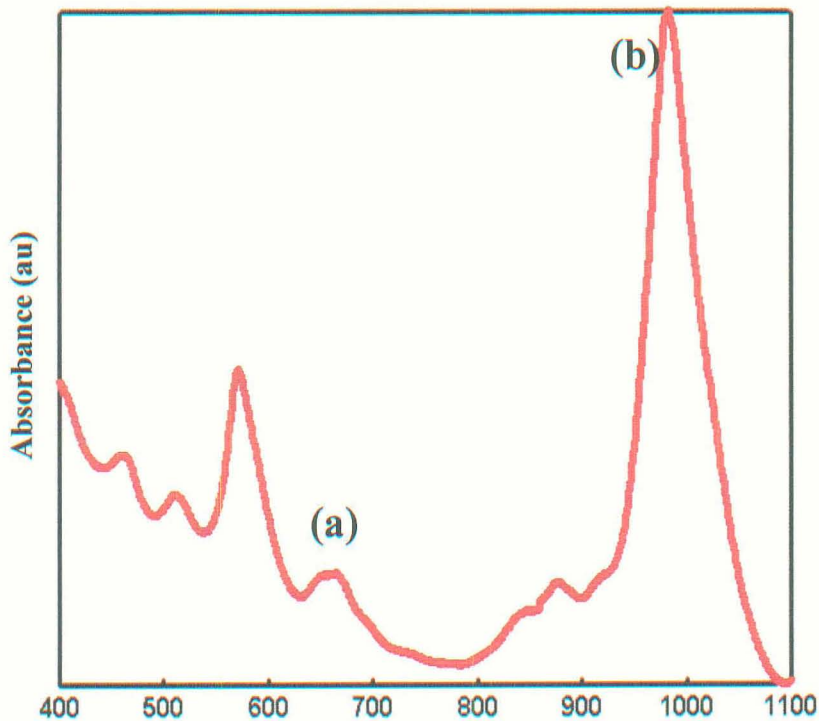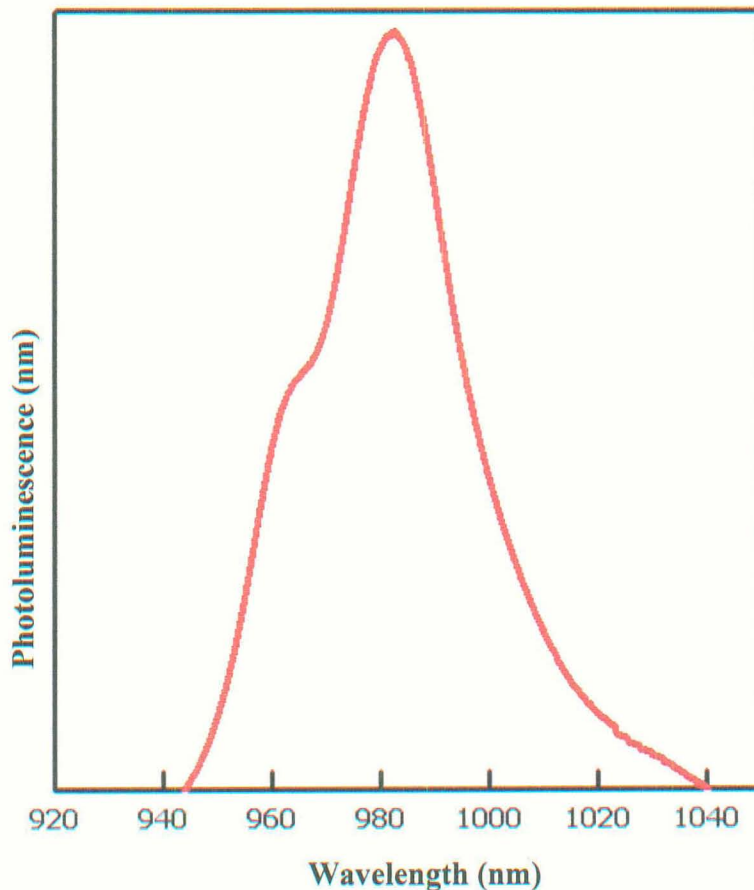**Figure 3.12 Photoluminescence spectra SC/CoMoCAT SWNTs**

The Figure 3.12 shows the emission spectra of sodium cholate encapsulated single walled carbon nanotubes. The sample was excited with 532 nm (2.33 eV) CW laser. A sharp, narrow, symmetric peak was observed at 988 nm. Comparison of the photoluminescence peak with the absorption spectrum reveals a striking correspondence. Thus the E_{11} transition of the (6, 5) tube was resolved in the photoluminescence spectra. A small bump was observed at 965 nm in the emission spectra. It could be an unresolved feature of the emission spectrum or a misalignment in the optical setup. The ripples observed at the end of the spectrum (between 1020 − 1040 nm) were due to the second harmonic generation of the laser excitation at 1062 nm.

(d) DNA encapsulated CoMoCAT tubes:

DNA is a naturally occurring polymer [36]. Molecular recognition between complementary strands of a double-stranded DNA could be used to construct various geometric objects at the nanometer scale. A large molecular library can be formed by single-stranded DNA (ssDNA), thus ssDNA can form π-stacking interactions with the side-wall of carbon nanotubes. ssDNA of "GT-GT-GT-GT" sequence, with 32 base pairs were used to wrap CoMoCAT single walled carbon nanotubes [36]. Dispersion of ssDNA and single walled carbon nanotubes was sonicated in an ice water bath to prevent the excess heating of DNA. Optical absorption and emission spectra provided evidence of individually dispersed carbon nanotubes. DNA wrapped individual single walled carbon nanotubes can be used for various biological applications such as, drug delivery, targeting and destroying particular cells, placing DNA wrapped carbon nanotubes inside cells

(CoMoCAT). Individual spectral features were obtained in the absorbance spectra. Absorbance spectra of DNA wrapped CoMoCAT single walled carbon nanotubes was not resolved as well compared to sodium cholate (SC) encapsulated CoMoCAT carbon nanotubes, however the emission spectra was reasobably well resolved. Absorbance spectra retained all the features, with two main peaks at 990 nm and 573 nm. We assign these two peak to the E_{11} and E_{22} transition of (6, 5) tube. The odd feature in the absorbance spectra at 860 nm was an instrumental error.
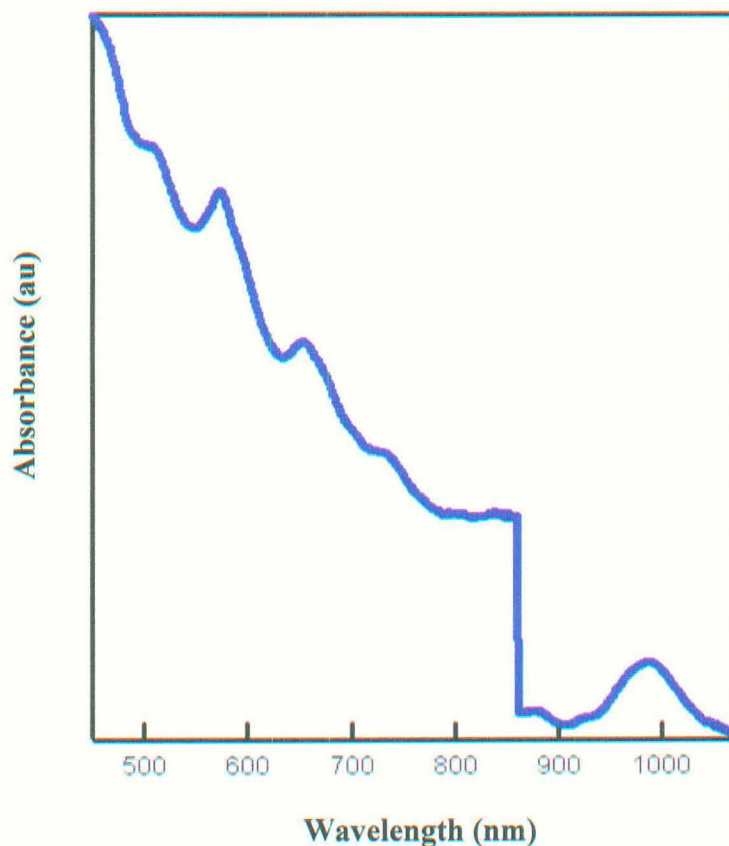
Figure 3.13 Absorbance spectra of DNA/CoMoCAT carbon nanotubes

Figure 3.14 shows the photoluminescence spectra of DNA wrapped CoMoCAT carbon nanotubes. A 532 nm (2.33 eV) CW laser source was used for excitation

of the sample. A sharp optical feature was obtained at 990 nm, which exactly coincides with the absorbance spectra at 990 nm. The emission feature was observed from the E_{11} transition of (6, 5) tube. The small bump observed at 965 nm in the emission spectra of sodium cholate encapsulated CoMoCAT carbon nanotubes, was observed in the DNA encapsulated CoMoCAT carbon nanotubes too, which again suggested that it could be an unresolved feature in the emission spectrum.
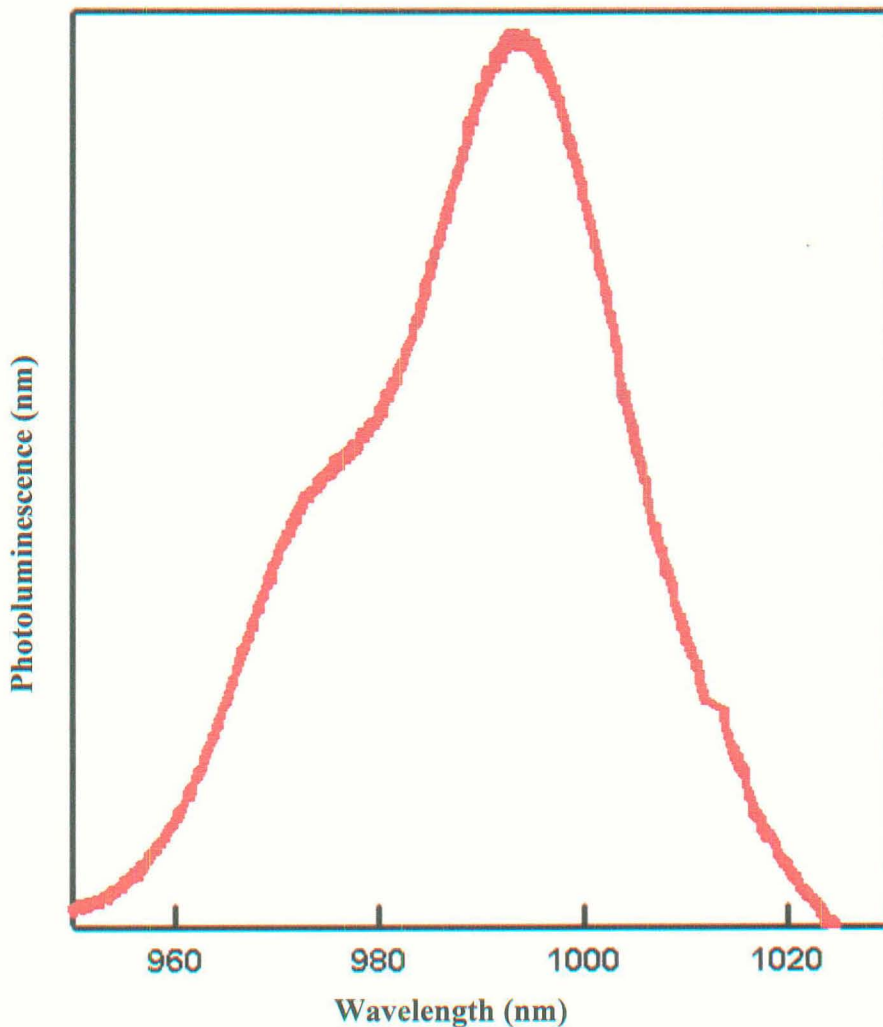
Figure 3.14 Photoluminescence spectra of ssDNA/CoMoCAT carbon nanotubes

However, it could even be an optical alignment issue. The small ripples observed towards the end of the emission spectrum between 1010 and 1020 are due to the second harmonic generation of the excitation laser source.

(e)Na-CMC encapsulated CoMoCAT carbon nanotubes:

Na-CMC (Sodium carboxyl methyl cellulose) is an etherified derivative of cellulose. Sodium salt of carboxyl-methyl group, it is commonly used as an emulsifier, for making gel and also used as an adhesive [39]. Na-CMC has an excellent quality of making thin, homogenous, uniform films by simply casting it on flat substrate such as glass [40]. Using Na-CMC as an encapsulant for carbon nanotubes, it was found that its dispersing ability was four times as high as any other encapsulant used in this study. Initial absorbance measurements did not reveal any optical features; it was only when the Na-CMC/CoMoCAT solution was diluted almost four times its initial concentration that significant optical absorbance in the sample. Figure 3.15 shows the absorbance spectra of Na-CMC/CoMoCAT carbon nanotubes solution (blue spectrum) and film (red spectrum). Excellent sharp, narrow and symmetric optical features were obtained in the absorbance spectra. As observed for (c) sodium cholate and (d) DNA encapsulated CoMoCAT carbon nanotubes, two sharp peaks at 573 nm and 990 were observed for Na-CMC/CoMoCAT carbon nanotubes. As seen in Figure 3.15, all the optical features observed in the absorbance spectra of the Na-CMC/SWNTs solution are retained in the absorbance spectra of Na-

CMC/SWNTs film. This confirms that no agglomeration or re-bundling of tubes took place during the thin film formation.
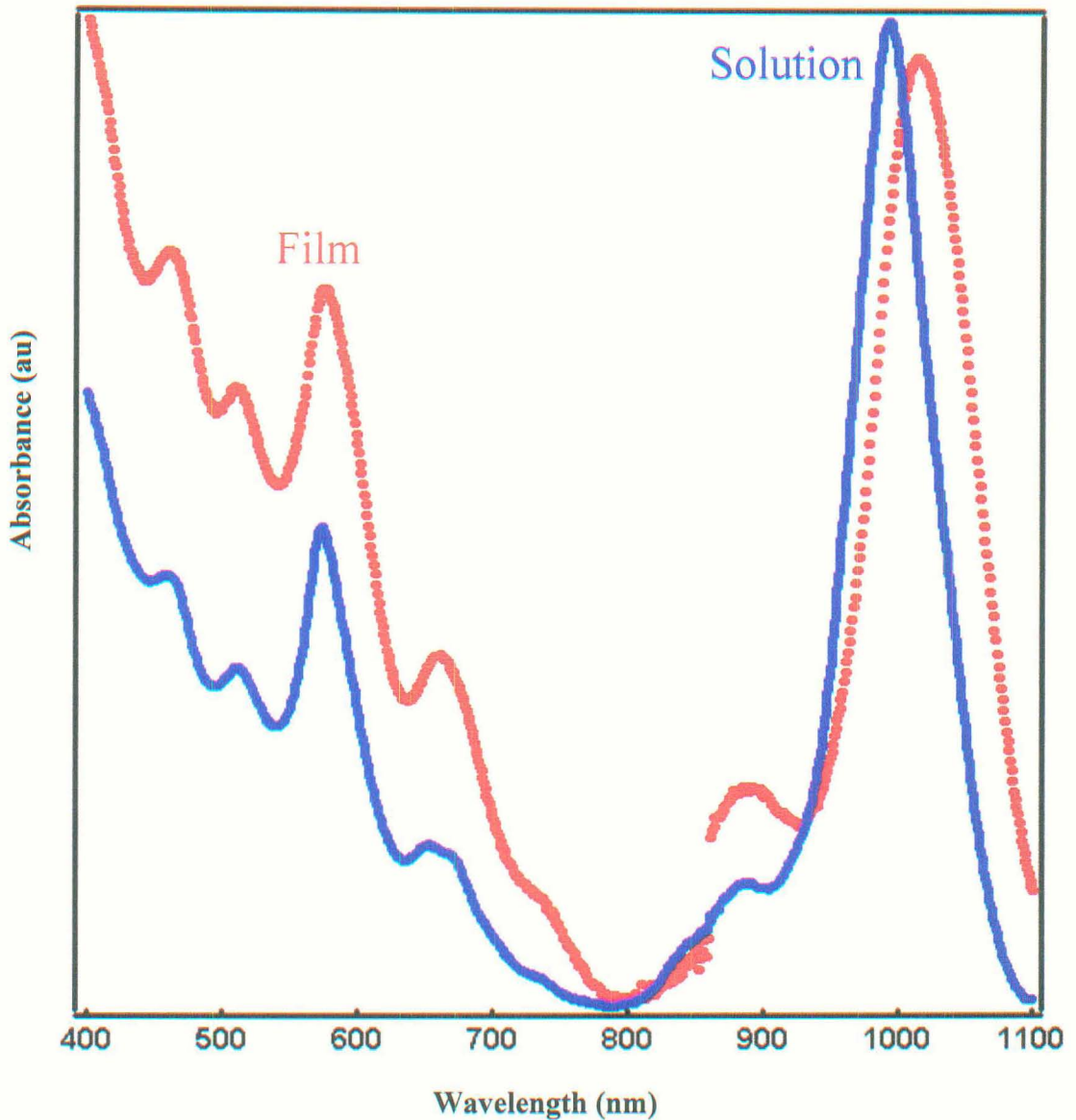
Figure 3.15 Absorbance spectra of Na-CMC/SWNTs solution and

film

It was also observed that the absorbance peak at 990 nm in the solution was slightly broadened and shifted (~ 10 nm) in the absorbance spectra of the film. Figure 3.16 shows the photoluminescence spectra of the solution (red spectrum) and the film (blue spectrum) of Na-CMC encapsulated carbon nanotubes. A

sharp, well structured featured structure was observed in the emission spectrum of the solution at 990 nm. The emission spectra of Na-CMC/SWNTs film showed a broad, asymmetric feature at 1000 nm. The emission spectra of the film confirm that isolation of carbon nanotubes was well preserved and maintained in the Na-CMC/SWNTs solid matrix. As seen in the Figure 3.16 the emission peak observed from Na-CMC/SWNTs film was shifted by 10 nm when compared with the emission feature from Na-CMC/SWNTs solution. This showed how sensitive carbon nanotubes were to there surrounding environment. The emission spectrum of Na-CMC/CoMoCAT carbon nanotubes film confirms that these films were optically active.
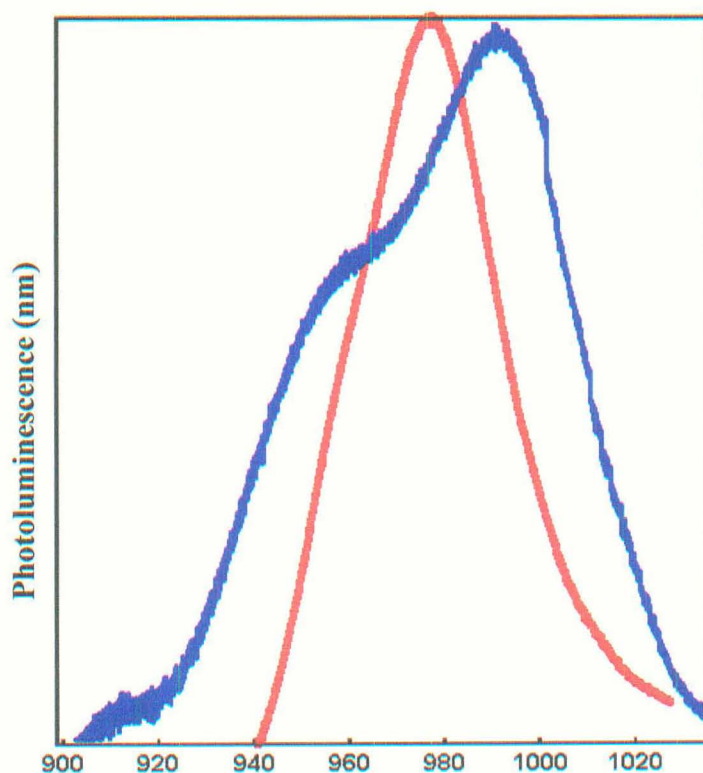
Figure 3.16 Photoluminescence spectra of Na-CMC/SWNTs solution and film

Wavelength (nm)

CHAPTER IV

SWNTs THIN FILM DEVICE FABRICATION AND MEASUREMENTS

Well aligned homogenous carbon nanotube films appear to be competitive with the electrically conducting layers used in video displays [41], solar cells [42], optical communication [43] equipment and other electronic applications. Other applications such as strain sensors [44], electroluminescent devices [45] would also be areas of interest. The pure nanotube films are almost transparent to infrared light, which makes these films potentially important for military applications such as smart sensors, infrared viewer etc. Transparent carbon nanotube films are better compared to commercially available transparent conducting thin films of ITO (Indium Tin Oxide) [46]. Flexible screens made with ITO, used in television and computer screens, fail because the material is brittle. However the nanotube films are much harder and could be a replacement for these materials. Agglomeration of tubes in these thin films is the main problem which prevents optical emission and absorption of light [10], various encapsulants used with appropriate sonication and centrifuge speeds could be used to prevent agglomeration of tubes. Single walled carbon nanotube thin films with excellent flatness and homogeneity were prepared using Na-CMC as encapsulant. The absorption spectrum of SWNT/Na-CMC film retains all almost all the spectral features of the standing solution except for slight broadening and a

shift in the peak positions (Figure 3.16). This shows that practically no agglomeration of nanotubes takes place during the film formation. Casting the SWNT/NaCMC solution on Silicon/Silicon Oxide substrates, thin films were prepared and photocurrent measurements were performed on these films.

4.1. Photocurrent Measurement:

Figure 4.1 shows the device schematic used for the experiment. All the photocurrent measurements were performed in air, at 300 K temperature. A thin, uniform Na-CMC/SWNTs film was deposited on a Si/SiO_2 substrate. The SiO_2 layer was 100 nm thick. 40 nm Au electrodes with 5 nm adhesion layer of Titanium were directly deposited on the film using an aluminum mask, leaving gap between the two electrodes.
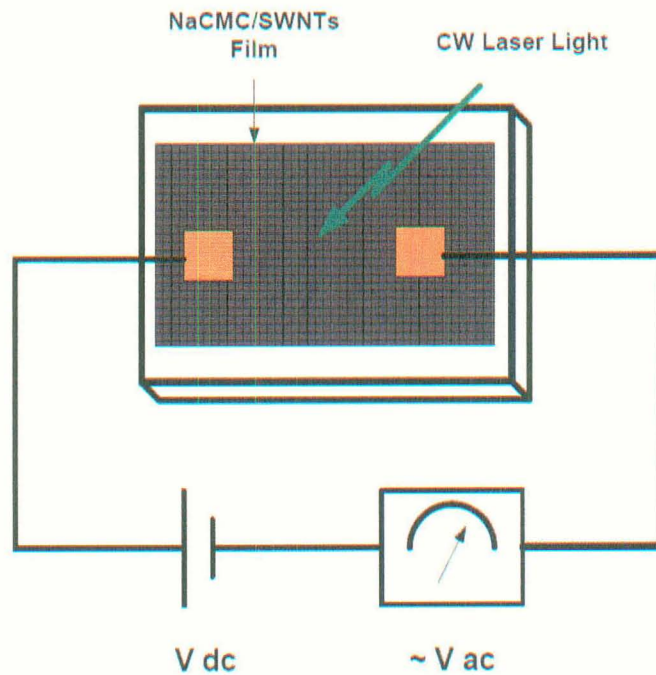
Fig 4.1 Device Schematic for Photocurrent measurement

As shown in Figure 4.1, the sample was biased at one electrode and photocurrent was measured from the other electrode. The laser was switched "ON" and "OFF" to measure the photocurrent signal. A continuous wave diode laser (532 nm excitation) was used as an illumination source. The laser power (300 mW) was kept constant during the entire experiment. The separation between the two electrodes was approximately 5000 microns. The thickness of the deposited film was ~ 20 microns. The device resistance was 110-120 M Ohms. The high device resistance is attributed to the low conductivity of Sodium carboxyl methyl cellulose [47].
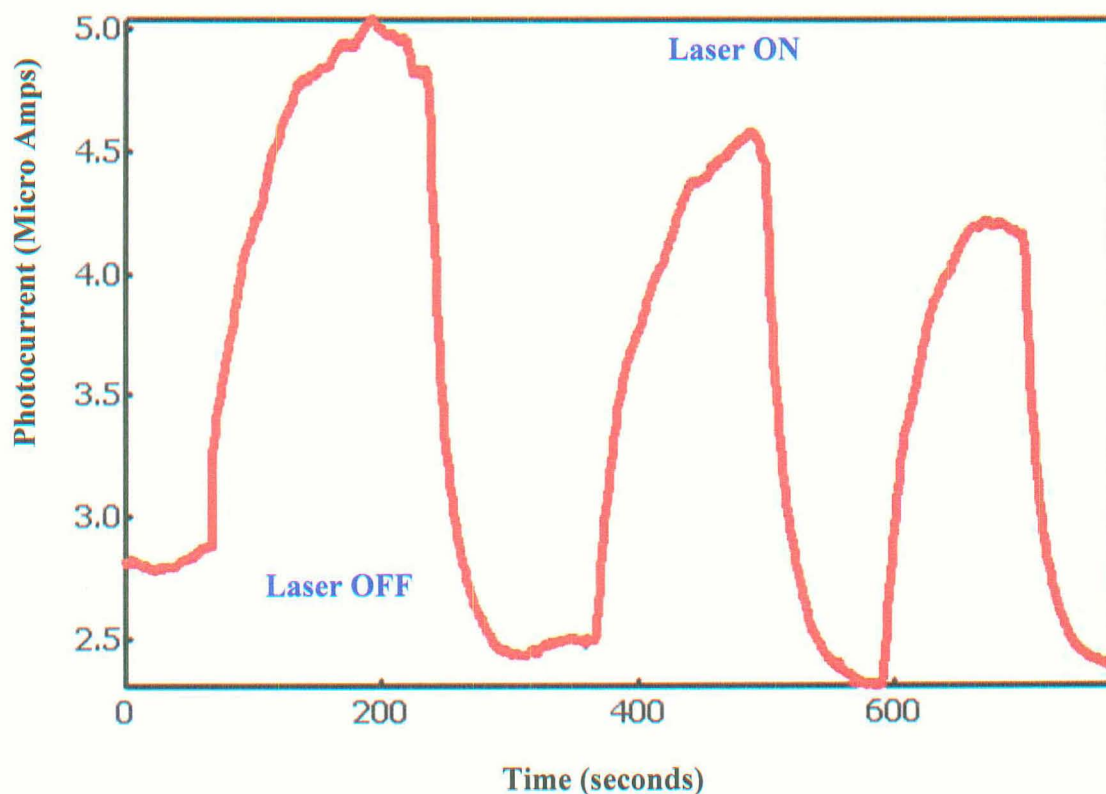
Fig 4.3 Photocurrent signal from Na-CMC/SWNTs film

When the carbon nanotubes were illuminated, photon energy was absorbed by the nanotubes, resulting in generation of electron-hole pairs. The observed

photocurrent response in carbon nanotubes would be most likely due to the excitation of charge carriers over the nanotube polymer barrier. The carriers which could overcome the nanotube polymer barrier could make it to the (Ti/Au) electrodes in the presence of an applied electric field. When no or a small electrical field was applied to the sample a very small signal was observed, however in the presence of an electrical field a significant photocurrent signal was measured. To confirm the photocurrent signal, the illumination source was switched ON and OFF. Figure 4.3 shows the observed photocurrent signal in the presence and absence of laser light source. An AC current technique was also performed to measure the photocurrent on the sample using a chopper. The sample was illuminated with the chopper operated at different frequencies. A significant photocurrent signal was observed at low frequencies (7 – 10 Hz). The sample exhibited a rapid decrease in photocurrent amplitude with increasing chopper frequency [48]. However a small photocurrent of approximately five micro amps was still seen when the laser frequency was increased to 200 Hz. Thus photon induced charge carrier generated in nanotubes and subsequent charge separation between the nanotube-polymer barrier and metal electrodes, believed to cause photoconductivity changes was studied. Larger contact area between the electrodes (~ 5 micron) was assumed to increase the carrier accumulation and photocurrent.

4.2 Thin film transistor fabrication and measurement:
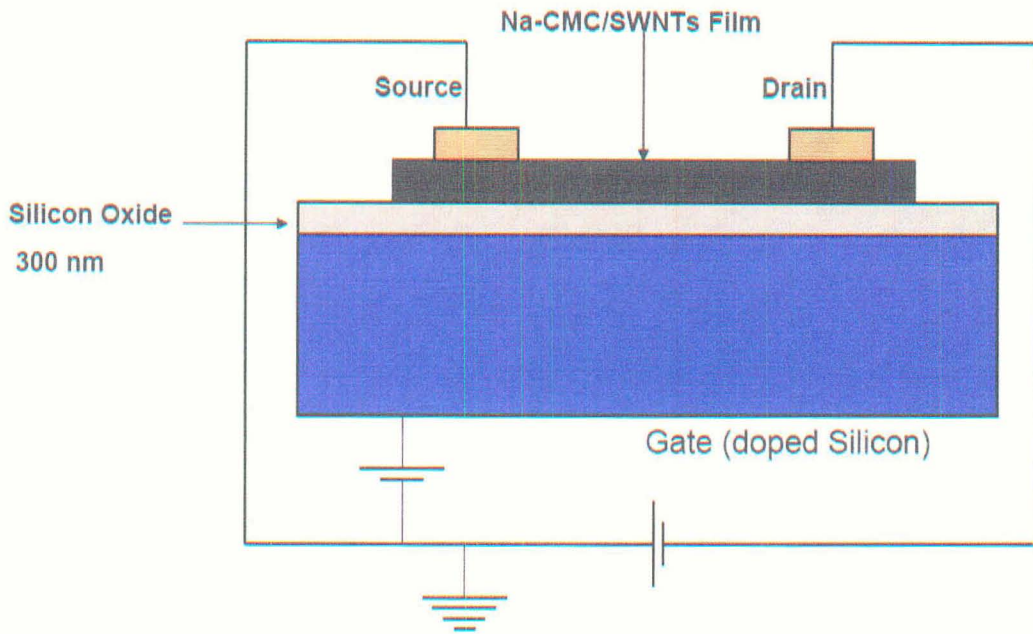
Fig 4.4 Schematic of Thin film transistor

Network of carbon nanotubes were used as a conducting channel in a thin film transistor (TFT) device. Figure 4.4 shows the device schematic of the fabricated TFT. All the measurements were performed in air and at 300K. The two electrodes (Ti/Au) were directly evaporated on the film, using an aluminum foil as a mask. Heavily doped silicon was used as a back gate. Figure 4.5 shows the gate dependence of the thin film transistor. Na-CMC/SWNTs thin films showed significant gate dependence. Gate voltage was varied from -9 to 9 volts. V_{DS} was fixed at 10 volts. The device switches "ON" at ~ -4 volts. The device demonstrates "ON" state when negative voltage is applied to it confirming that

the majority charge carriers in this channel are holes. Thus the device exhibits a p-type semiconducting behavior at room temperature.

Fig 4.5 Current-Voltage characteristics of the TFT

CHAPTER V

CONCLUSION

Different encapsulant wrapped single walled carbon nanotubes were suspended in liquid solutions. Optical spectroscopic measurements including Raman, absorbance and photoluminescence were performed on these samples. Using the theoretical predictions, Radial breathing mode (RBM) in Raman measurements helped determine the diameter distribution of single walled carbon nanotub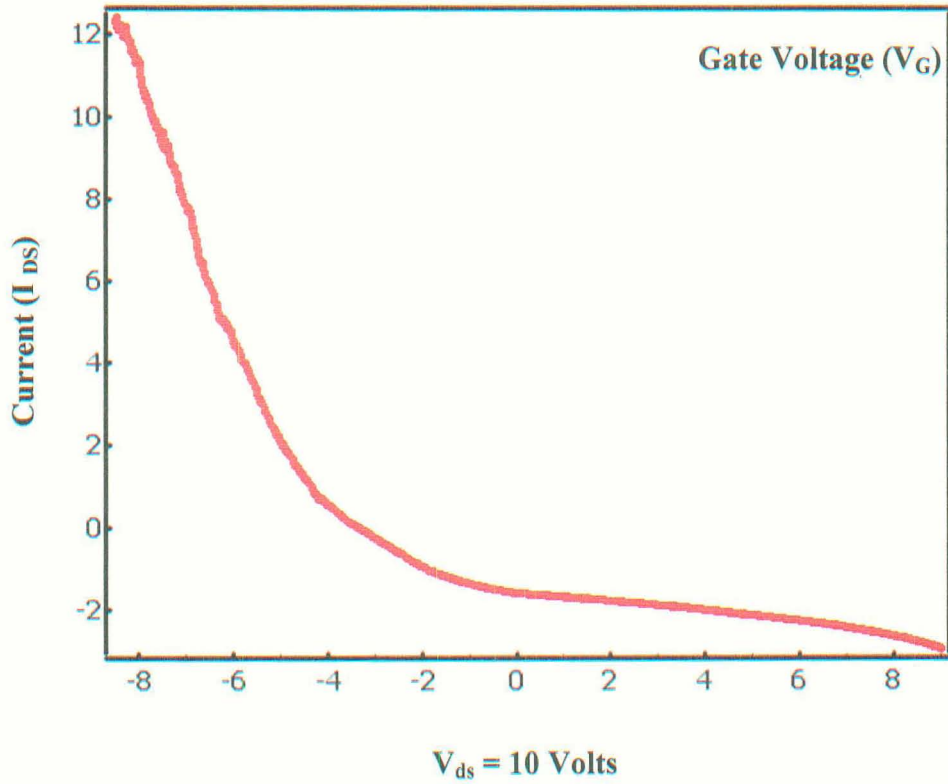es. Bright spectral features attributed to the superposition of distinct electronic transitions from a variety of individual fullerene nanotubes were observed in the absorbance measurements in visible and near infra red. Bright infra red emission was observed from these individually suspended tubes in liquid solution as well as from the thin films of carbon nanotubes. Using the band-gap energy spacing and the tight binding model, the (n, m) values were assigned to different tubes.

Thin films of carbon nanotubes which retained all the spectral features of the liquid solution in the absorbance and photoluminescence spectrum were fabricated. This confirmed that no aggregation of re-bundling of tubes took place during the thin film formation. These optically active films of single walled carbon nanotubes were used for photocurrent measurements. A significant photocurrent signal was obtained by illuminating the sample with an excitation source (CW Diode laser 532 nm). Photocurrent signal was attributed to the carriers generated from individual/networks of carbon nanotubes. Thin film

transistors were fabricated using these SWNTs films. These films showed significant gate dependence. The TFT (thin film transistor) switched "ON" when negative voltage was applied to it.

Future experiments such as density gradient ultracentrifugation (DGU), which helps separation of carbon nanotubes based on there electronic structure (metallic or semiconducting tubes) would be an interesting extension of this research. Thin films of carbon nanotubes can be used for interesting future experiments such as strain sensor and electroluminescent devices. Electroluminescence device using thin films of carbon nanotubes would be a very interesting idea for direct industry application.

REFERENCES

1. M.M.T. Treacy, T.W. Ebbesen and J.M. Givson, *Nature* 381 (1996), p. 678.

2. P. M. Ajayan and O. Zhou, "Applications of carbon nanotubes", in Carbon Nanotubes Synthesis, Structure, Properties and Applications (eds. M. S. Dresselhaus, G. Dresselhausand Ph. Avouris), *Springer Publications* (2001). (Book Chapter).

3. L. X. Zheng, M. J. O'Connell, S. K. Doorn, X. Z. Liao, Y. H. Zhao, E. A. Akhadov, M. A. Hoffbauer, B. J. Roop, Q. X. Jia, R. C. Dye, D. E. Peterson, S. M. Huang, J. Liu and Y. T. Zhu, *Nature Materials* 3, 673 - 676 (2004).

4. Iijima, S. Helical Microtubules of Graphitic Carbon. *Nature*, 1991, *354*, 56.

5. R. Bacon. "Growth, Structure and properties of Graphite Whiskers." *J.Appl. Phys.* 31 383 (1960).

6. Iijima, S.; Ichihashi, T. Single-shell Carbon Nanotubes of 1-nm diameter. *Nature* 1993, *363*, 603.

7. Bethune, D.S.; Kiang, C.H.; de Vries, M.S.; Gorman, G.; Savoy, R.; Vasquez, J.; Beyers, R. Cobalt-catalyzed Growth of Carbon Nanotubes with Single-Atomic- Layer Walls. *Nature* 1993, *363*, 605.

8. A.Thess, R. Lee, P. Nikolaev, H. Dai, P. Petit, J. Robert, C. Xu, Y. H. Lee, S. G. Kim,A. G. Rinzler, D. T. Colbert, G. E. Scuseria, D. Tománek, J. E. Fischer, and R. E.Smalley. "Crystalline Ropes of Metallic Carbon Nanotubes" *Science* 26 July 1996; 273: 483-487.

9. L.A.Girifalco, M.Hodak, R.S.Lee, *Phys. Rev. B* 62, 13104 (2000).

10. Michael J. O'Connell, Sergei M. Bachilo, Chad B. Huffman, Valerie C. Moore, Michael S. Strano, Erik H. Haroz, Kristy L. Rialon, Peter J. Boul, William H. Noon, Carter Kittrell, Jianpeng Ma, Robert H. Hauge, R. Bruce Weisman, Richard E. Smalley *Science* 297, 593 (2002).

11. R. Saito, G. Dresselhaus, M.S.Dresselhaus, *Physical properties of carbon nanotubes* (Imperial College press, London, 1998).

12. Jeroen W .G. Wilder, Liesbeth C. Venema, Andrew G. Rinzler, Richard E. Smalley; Cees Dekker, Nature 391, 6662, 59-62 (1998).

13. M. A. Pimenta, A. Marucci, S.D.M. Brown and M.J. Matthews, A. M. Rao, P. C. Eklund, R. E. Smalley, G. Dresselhaus, M. Dresselhaus, *Journal of Materials Research* 13, 9 (1998).

14. R. Saito, T. Takeya, T. Kimura, G. Dresselhaus and M. S. Dresselhaus, *Physical Review. B* 57, 4145 (1998).

15. S. Bandow, S. Asaka, Y. Saito, A. M. Rao, L. Grigorian, E. Richter, and P. C. Eklund, *Physical Review Letter* 80, 3779 (1998).

16. H. Kataura, Y. Kumazawa, Y. Maniwa, I. Umezu, S. Suzuki, Y.Ohtsuka, and Y. Achiba, *Synthetic Materials*. 103, 2555 (1999).

17. L. Alvarez, A. Righi, T. Guillard, S. Rols, E. Anglaret, D.Laplaze, and J.-L. Sauvajol, *Chemical Physical Letters*. 316, 186 (2000).

18. S. D. M. Brown, A. Jorio, P. Corio, M. S. Dresselhaus, G.Dresselhaus, R. Saito, and K. Kneipp, *Physical Review B* 63, 155414 (2001).

19. Sergei M. Bachilo, Michael S. Strano, Carter Kittrell, Robert H.Hauge, Richard E. Smalley, R. Bruce Weisman, *Science* 298, 2361 (2002).

20. J. Lefebvre, J. M. Fraser, Y. Homma and P. Finnie, *Applied Physics A: Materials Science and Processing* 78, 8 (2004).

21. L. A. Girifalco, M. Hodak, R. S. Lee, *Physical Review B* 62, 12104 (2000).

22. Carbon Nanotubes: Synthesis, Structure Properties and Applications; Dresselhaus, M. S. Dressalhaus, G. Avouris, Ph. Eds.; Springer –Verlag: Berlin, (2001).

23. Special issue on carbon nanotubes; *Physics World*, 13 (6), June (2000).

24. Collins, P. G, Avouris Ph., Nanotubes for Electronics, *Scientific America.* (2000), 283, 38-45.

25. Tans, s. Verschueren, S, dekkee: C. Room-Temperature Transistor Based on single Carbon nanotube. *Nature* (London) 393, 49 (1998).

26. Martel, R,;Schmidt,T,;Shea,H.R.; Hertel,T.;Avouris, Ph.;Single and Multi-Wall Carbon Nanotube Field-Effect Transistors, *Applied physics letters* 73, 2447 (1998).

27. Michael S. Arnold, Alexander A. Green, James F. Hulvat, Samuel I. Stupp and Mark C. Hersam, *Nature Nanotechnology* 1, 60 (2006).

28. Olga Matarredona, Heather Rhoads, Zhongrui Li, Jeffrey H. Harwell, Leandro Balzano and Daniel E. Resasco, *J. Phys. Chem. B 107,* 13357 (2003).

29. S.G. Chou, H.B. Ribeiro, E.B. Barros, A.P. Santos, D. Nezich, Ge.G. Samsonidze, C. Fantini, M.A. Pimenta, A. Jorio, F. Plentz Filho, M.S. Dresselhaus, G. Dresselhaus, R. Saito, M. Zheng, G.B. Onoa, E.D. Semke, A.K. Swan, M.S. Ünlü and B.B. Goldberg. *Chemical Physical Letters*, 397, 296 (2004).

30. Michael J. O'Connell, Ezra. E. Eibergen and Stephen K. Doorn, *Nature*, 4, 412.

31. Valerie C. Moore, Michael S. Strano, Erik H. Haroz, Robert H. Hauge, Richard E. Smalley, *Nanoletters,* 3, 1379 (2003).

32. Christie M. Sayes, Feng Liang, Jared L. Hudson, Joe Mendez, Wenhua Gu, Jonathan M. Beach, Valerie C. Moore, Condell D. Doyle, Jennifer L. West, W. Edward Billups, Kevin D. Ausman, Vicki LColvin, *Toxicology Letters* 161, 135 (2006).

33. Win Wenseleers, Igor I. Vlasov, Etienne Goovaerts, Elena D. Obraztsova, Anatolii S. Labach, August Bouwen, Advanced Functional Materials, 14, 1105 (2004).

34. A. Roda, A.F. Hofmann, K. J. Mysels, *Journal of Biological Chemistry*, 258, 6362 (1983).

35. P.J. Collings, J.S.Patel, *Handbook of Liquid Crystal Research*, Oxford University Press, New York 1997.

36. Ming Zheng, Anand Jagota, Ellen D. Semke, Bruce A. Diner, Robert D. Mclean, Steve R. Lustig, Raymond E. Richardson, Nancy G. Tassi, *Nature Materials*, 2, 338 (2003).

37. Alberto Bianco, Kostas Kostarelos and Maurizio Prato, *Current Opinion in Chemical Biology*, 9, 674 (2005).

38. Nadine Wong Shi Kam, Michael O'Connell, Jeffrey A. Wisdom, and Hongjie Dai, *Proceeding of the National academy of Sciences*, 102, 11600, (2005).

39. J. I. Kroschwitz, ed., *Encyclopedia of Polymer Science and Engineering,* Vol. 3, John Wiley & Sons, Inc., 1985.

40. Nobutsugu Minami, yeji Kim, Kanae Miyashita, Said Kazoui, Balakrishnan Nalini, *Applied Physics Letters*, 88, 093123 (2006).

41. Chang-chun Zhu, Weihua Liu, Lujiang Huangfu, *J. Vac. Sci. Technol. B* (19) 5, 2001.

42. Brian J. Landi, Ryne P. Raffaelle, Stephanie L. Castro, Sheila G. Bailey, *Progress in Photovoltaics,* 13(2), 2005.

43. Y.-C. Chen, N. R. Raravikar, L. S. Schadler, P. M. Ajayan, Y.P. Zhao, T.M. Lu, G.C. Wang, X.C. Zhang, *Applied Physics Letters,* 81 (6), 2002.

44. Kenneth J. Loh, Jerome P. Lynch, Nicholas A. Kotov, *Proceedings of the 5th International Workshop on Structural Health Monitoring, Stanford, CA, USA, September 12-14, 2005.*

45. S. Kazaoui,a_ N. Minami, B. Nalini, and Y. Kim, N. Takada and K. Hara, *Applied Physics Letters,* 87, 211914 (2005).

46. Aurelien Du Pasquier, Husnu Emrah Unalan, Alokik Kanwal, Steve Miller, and Manish Chhowalla, *Applied Physics Letters*, 87, 203511 (2005).

47. Mohamed M. Abdel Moteleb, *Polymer Bulletin* 28, 689-695 (1992).

48. Shaoxin Lu, Balaji Panchapakesan, *Nanotechnology*, 17 1843 (2006).

CURRICULUM VITAE

Name: Hemant M. Shah

Address: Department of Electrical and Computer Engineering

                University of Louisville, Louisville, Kentucky 40292.

DOB: May 11th, 1981

Education:

    (a) Bachelor of Science from Maharaja Sayajirao University 2003

       Major: Instrumentation Engineering

    (b) Post Graduate Diploma from Maharaja Sayajirao University 2004

       Major: Solid State Electronics